ISSN 2096-7071
CN 10-1629/R1

CHINA CDC WEEKLY

Vol. 3 No. 41 Oct. 8, 2021

CCDC weekly

中国疾病预防控制中心周报

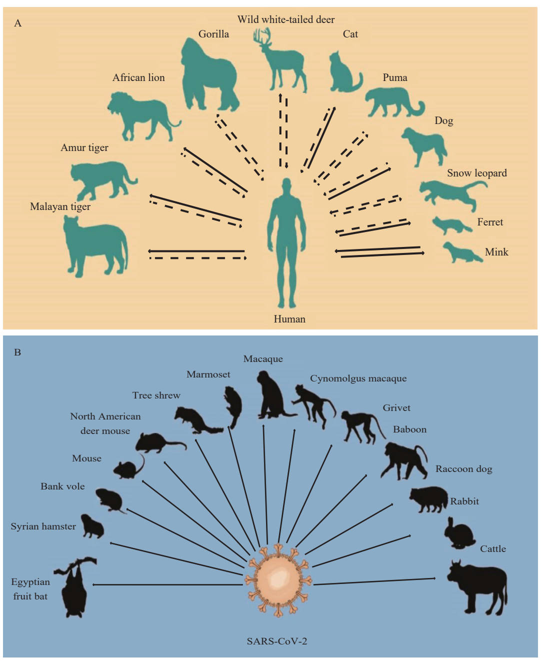

COVID-19 ISSUE (19)

Perspectives

COVID-19 Expands Its Territories from Humans to Animals 855

Targeted Prevention and Control of Key Links in Airports to Mitigate Public Health Risks 859

Outbreak Reports

Eleven COVID-19 Outbreaks with Local Transmissions Caused by the Imported SARS-CoV-2 Delta VOC — China, July–August, 2021 863

Methods and Applications

Braking Force Model on Virus Transmission to Evaluate Interventions Including the Administration of COVID-19 Vaccines — Worldwide, 2019–2021 869

ISSN 2096-7071
9 772096 707217 4 1>

Cover Image: Current known host range of SARS-CoV-2. (A) Species that have been reported to be infected by SARS-CoV-2 in nature. (B) Species that have reportedly been infected by SARS-CoV-2 via infection experiments.

Perspectives

COVID-19 Expands Its Territories from Humans to Animals

George F. Gao[1,2,#]; Liang Wang[2]

THE GLOBAL STATUS OF COVID-19 PANDEMIC

Since the discovery of a novel type of coronavirus named severe acute respiratory syndrome coronavirus 2 (SARS-CoV-2, also known as 2019-nCoV, or HCoV-19) (*1*), the causative agent of coronavirus disease 2019 (COVID-19), COVID-19 has been spreading globally during a short period of time. As of August 17, COVID-19 had caused more than 206 million infections, of which more than 4 million had died worldwide (*2*), which is the worst pandemic caused by coronaviruses thus far. The pandemic of COVID-19 has not only posed a global threat to public health but has also thoroughly taxed medical systems and global economies. In response to this pandemic, unprecedented efforts have been made worldwide, such as the implementation of non-pharmacological interventions (NPIs) (*3*) and vaccine development (*4*). However, several types of variants of concern (VOC) have been found gradually during the circulation of SARS-CoV-2, as the combination effects of their intrinsic characteristics of error-prone replication process, host immune pressure and other environmental factors. Several studies have documented that these VOCs showed increased transmissibility and were more resistant to neutralization by convalescent and vaccine sera than other variants, posing a global threat to public health. Taken together, the arms race between SARS-CoV-2 evolution and human coping strategies will continue for some time to come.

THE ORIGIN OF SARS-CoV-2 REMAINS A MYSTERY

For any causative agent of a pandemic, tracing the origin of the "prime criminal" is crucial for both understanding its evolution and preventing outbreaks in the future. To our knowledge, a bat-origin coronavirus RaTG13 had the most similar genome compared to SARS-CoV-2 at the whole genomic level (96.2%), although the amino acid similarity of the receptor binding domain (RBD) of the spike protein, which mediates the viral entry to human cell, was only 89.2%. RaTG13 pseudovirus could transduce cells expressing human ACE2 with low efficiency (*5*). Subsequently, several coronavirus genomic sequences with high similarity to SARS-CoV-2 from bats have been found in different countries (*6*–*8*). Both pseudotyped SARS-CoV-2 virus and wild SARS-CoV-2 virus could infect cells expressing ACE2 from *Rhinolophus macrotis* (*9*). These results indicated that SARS-CoV-2 could have more likely originated from bats. However, it is well established that intermediate hosts are needed for bat-origin coronaviruses before they acquire sufficient mutations to have the ability to infect humans, such as dromedary camels for MERS-CoV. Two groups reported that they found SARS-CoV-2-related coronaviruses in Malayan pangolins (*Manis javanica*) and their RBD region had a high similarity to that of SARS-CoV-2. Yet, the overall genomic similarity compared to SARS-CoV-2 were both low (<93%), which suggested pangolins were unlikely to be the intermediate host for SARS-CoV-2. So far, the mysteries of the route through which SARS-CoV-2-related coronaviruses were transmitted from bats to humans and if bats were the original reservoir host still remain unsolved.

THE SPILLOVER OF SARS-CoV-2 EVENTS AND THEIR POTENTIAL MOLECULAR MECHANISMS

In addition to humans, natural infection of SARS-CoV-2 have been found in several other species of mammals via contact with COVID-19 patients, such as cats, dogs, lions and tigers in zoos, minks, and ferrets (*10*) (Figure 1A). Snow leopards, pumas, and gorilla also have been found to be infected with SARS-CoV-2 in nature (*10*) (Figure 1A). Among these spillover events, mink-related SARS-CoV-2 variants had the greatest impact, as the mink had also transmitted the SARS-CoV-2 variants back to humans and caused

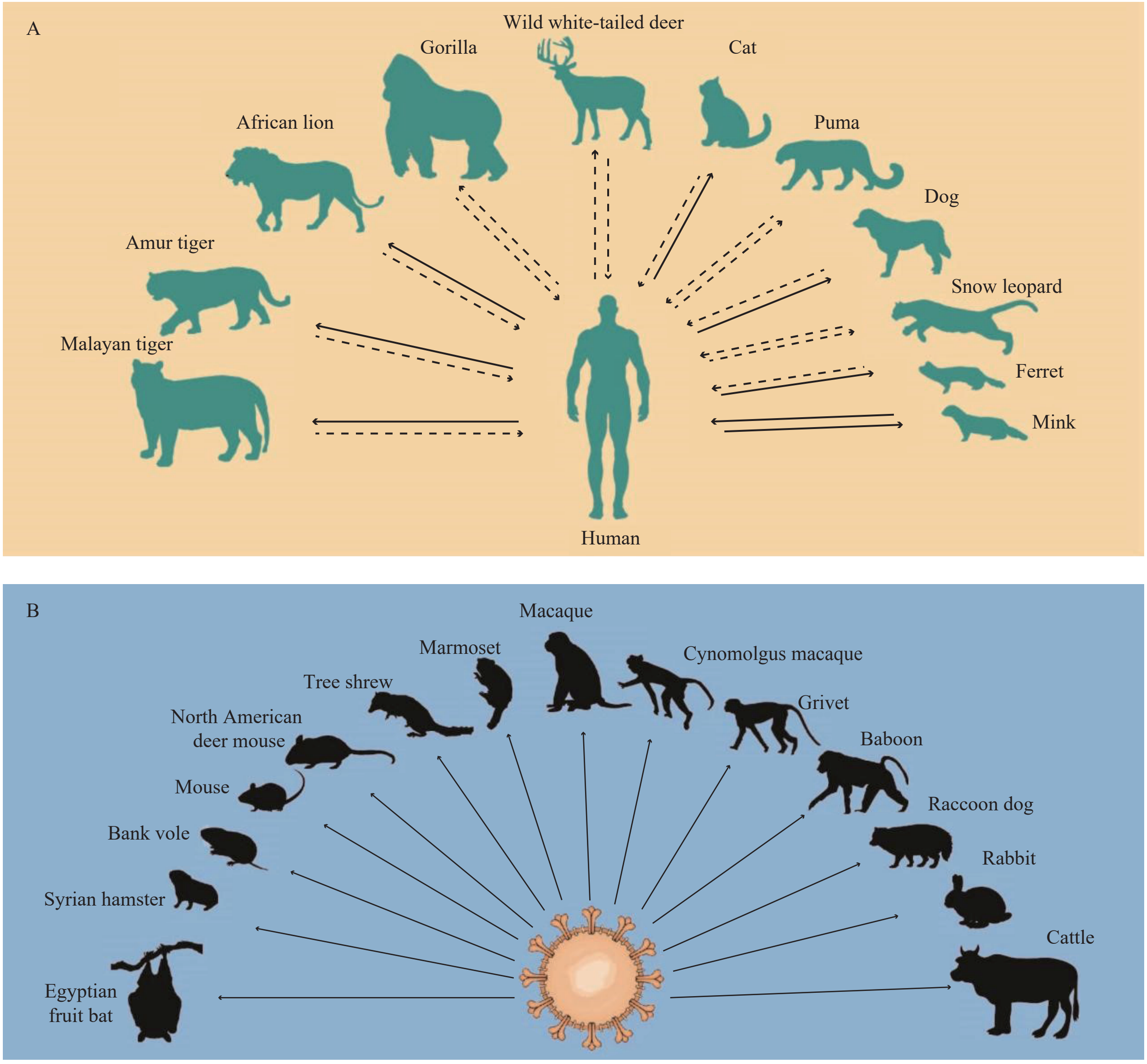

FIGURE 1. The currently known host range of SARS-CoV-2. (A) Species that have been reported to be infected by SARS-CoV-2 in nature. (B) Species that have reportedly been infected by SARS-CoV-2 via infection experiments.
Note: A solid arrow indicates that there is clear evidence showing the cross-species transmission direction of SARS-CoV-2, while a dashed arrow indicates a possible cross-species transmission direction of SARS-CoV-2.

further community transmission (*11*). In order to prevent the mink-derived SARS-CoV-2 variants from continuously both circulating in the minks and spreading to humans, tens of millions of minks have been culled which also caused huge economic losses to mink-related industries. In addition to natural infection cases, several animals (e.g., rabbits, pigs, foxes, and civets etc.) have also been considered as possibly susceptible hosts of SARS-CoV-2 through infection experiments (*10*) (Figure 1B). Although most natural infections described above occurred in domesticated animals, far fewer cases were identified in the wild.

Recently, serosurveillance showed that antibodies against SARS-CoV-2 have been found in 40% of samples of wild white-tailed deer (*Odocoileus virginianus*) from USA in 2021 (*12*). However, antibodies were detected in only 1 and 3 samples from 2019 and 2020, respectively (*12*). Although it is still not known if SARS-CoV-2 in wild white-tailed deer was introduced by humans, the significant increase of positive rate of antibodies indicated that SARS-CoV-2 had been circulating in wild white-tailed deer. Due to the wide geographic distribution and large population (approximately 30 million) of wild white-tailed deer in North America, contact between human and wild white-tailed deer could be achieved by several activities such as wildlife rehabilitation, field research, practical conservation work and some wildlife-related tourism, supplemental feeding, captive cervid operations, and hunting (*13*). In this case, it increased the risk that SARS-CoV-2 from wildlife would spillback to humans.

Structural and functional studies identified several key sites from both SARS-CoV-2-RBD and ACE2. Mutations at these sites are closely related to the cross-species transmission of SARS-CoV-2. On SARS-CoV-2-RBD, residues 493, 498, and 501 were identified as key mutation hotpots that determine the host range. Mouse-adapted strains with N501Y mutation on RBD were isolated after 6 passages cultured in aged mice by wild type SARS-CoV-2 (*14*). Another 2 mutations, namely Q493K and Q498H were introduced to the S protein in mouse-adapted strains. Retrospective analysis showed that Q493K began to appear after 5 passages and, notably, Q498H dominated after only 1 passage. On ACE2, residues 41 and 42 were recognized as the critical sites for SARS-CoV-2 RBD binding. Sequence alignment showed that these two residues account for the major difference in the interaction network with SARS-CoV-2 RBD among different ACE2 orthologs (*9*). There are 4 combinations at these 2 sites (Y41-Q42, H41-Q42, Y41-E42, and H41-E42). Among them, Y41-Q42 combination showed the highest binding affinity to SARS-CoV-2 RBD; H41-Q42 showed much weaker; Y41-E42 was weaker than that of H41-Q42; and H41-E42 showed the weakest binding to SARS-CoV-2 RBD. In addition, K31 and K353 have been reported as a hotspot providing substantial amount of energy in receptor binding, and the mutation from K353 to A353 may abolish the binding capacity of ACE2 to SARS-CoV-2-RBD.

THE HOST EXPANSION OF SARS-CoV-2 IS NOT OVER

The host expansion of coronaviruses was well established (*15*). A previous study found some ongoing mink-adapted mutations such as Y453F, F486L, and N501T in the S protein; for example, Y453F has been found to increase in hACE-2 affinity (*16*). Those results suggested that some ongoing mink-adapted mutations posed a huge threat to public health if they transmitted back to humans and even triggered further community transmission. Due to the fact that minks are bred in farms, large-scale slaughter of these minks can effectively prevent mink-derived SARS-CoV-2 variants from spreading and mutation accumulation in the mink population. However, similar measures could not be taken for wild animals. Together with the fact that adaptive mutations are needed when cross-species transmission happens and then circulate among populations of the new host, more efforts are needed to survey the genetic alterations and corresponding impact of transmissibility and infectivity in humans in these novel variants from wild white-tailed deer. Since SARS-CoV-2 is going wild, many other wild animals would also be infected with SARS-CoV-2 via direct or indirect contact with wild white-tailed deer or even infected patients. Several experimental studies have demonstrated several animals could be susceptible to SARS-CoV-2, such as Egyptian fruit bats (*Rousettus aegyptiacus*), marmosets (*Callithrix jacchus*), macaques (*Macaca fascicularis* and *Macaca mulatta*), bank voles (*Myodes glareolus*), and North American deer mice (*Peromyscus maniculatus*) (*10*). However, these are just the tip of the iceberg as the susceptibility of most terrestrial wild animals to SARS-CoV-2 has not been tested. In addition, the research on susceptibility of marine wildlife (especially marine mammals) to SARS-CoV-2 is still lacking. Due to frequent marine human activities (such as mariculture and marine fishing), the frequency of human contact with marine organisms is high. If some marine organisms are highly susceptible to SARS-CoV-2, there is a risk that SARS-CoV-2 could be transmitted from humans to marine organisms, and worse, SARS-CoV-2 then might spread in the marine ecosystem, which may lead to the generation of some novel SARS-CoV-2 variants with unknown threats to humans. Therefore, it is necessary to carry out large-scale SARS-CoV-2 screening for terrestrial and marine wildlife, especially those susceptible ones, in order to monitor the status of infection and mutation of SARS-CoV-2 in wild animals, so as to formulate further prevention and control strategies. It also provides more clues to the study of the origin and cross-species transmission of SARS-CoV-2.

Acknowledgement: Dr. Kefang Liu and Mr. Linjie Li for help in collecting the references and drawing figure.

Funding: Supported by the Strategic Priority Research Program of the Chinese Academy of Sciences (XDB29010202) and the intramural special grant for SARS-CoV-2 research from the Chinese Academy of Sciences.

doi: 10.46234/ccdcw2021.210

Corresponding author: George F. Gao, gaof@im.ac.cn.

[1] Chinese Center for Disease Control and Prevention, Beijing, China; [2] CAS Key Laboratory of Pathogen Microbiology and Immunology, Institute of Microbiology, Center for Influenza Research and Early-warning, CAS-TWAS Center of Excellence for Emerging Infectious Diseases, Chinese Academy of Sciences, Beijing, China.

Submitted: August 24, 2021; Accepted: September 06, 2021

REFERENCES

1. Tan WJ, Zhao X, Ma XJ, Wang WL, Niu PH, Xu WB, et al. A novel coronavirus genome identified in a cluster of pneumonia cases — Wuhan, China 2019–2020. China CDC Wkly 2020;2(4):61 – 2. http://dx.doi.org/10.46234/ccdcw2020.017.
2. World Health Organization. Coronavirus disease (COVID-19) weekly epidemiological update and weekly operational update. 2021. https://www.who.int/emergencies/diseases/novel-coronavirus-2019/situation-reports. [2021-08-05].
3. Li ZJ, Chen QL, Feng LZ, Rodewald L, Xia YY, Yu HL, et al. Active case finding with case management: the key to tackling the COVID-19 pandemic. Lancet 2020;396(10243):63 – 70. http://dx.doi.org/10.1016/S0140-6736(20)31278-2.
4. Dai LP, Gao GF. Viral targets for vaccines against COVID-19. Nat Rev Immunol 2021;21(2):73 – 82. http://dx.doi.org/10.1038/s41577-020-00480-0.
5. Liu KF, Pan XQ, Li LJ, Yu F, Zheng AQ, Du P, et al. Binding and molecular basis of the bat coronavirus RaTG13 virus to ACE2 in humans and other species. Cell 2021;184(13):3438 – 51.e10. http://dx.doi.org/10.1016/j.cell.2021.05.031.
6. Murakami S, Kitamura T, Suzuki J, Sato R, Aoi T, Fujii M, et al. Detection and characterization of bat Sarbecovirus phylogenetically related to SARS-CoV-2, Japan. Emerg Infect Dis 2020;26(12):3025 – 9. http://dx.doi.org/10.3201/eid2612.203386.
7. Hul V, Delaune D, Karlsson EA, Hassanin A, Tey PO, Baidaliuk A, et al. A novel SARS-CoV-2 related coronavirus in bats from Cambodia. bioRxiv, 2021. http://dx.doi.org/10.1101/2021.01.26.428212.
8. Zhou H, Ji JK, Chen X, Bi YH, Li J, Wang QH, et al. Identification of novel bat coronaviruses sheds light on the evolutionary origins of SARS-CoV-2 and related viruses. Cell 2021;184(17):4380 – 91.e14. http://dx.doi.org/10.1016/J.CELL.2021.06.008.
9. Liu KF, Tan SG, Niu S, Wang J, Wu LL, Sun H, et al. Cross-species recognition of SARS-CoV-2 to bat ACE2. Proc Natl Acad Sci USA 2021;118(1):e2020216118. http://dx.doi.org/10.1073/PNAS.2020216118.
10. World Organization for Animal Health. Infection with SARS-CoV-2 in animals. 2021. https://www.oie.int/app/uploads/2021/05/en-factsheet-sars-cov-2.pdf.[2021-08-05].
11. Munnink BBO, Sikkema RS, Nieuwenhuijse DF, Molenaar RJ, Munger E, Molenkamp R, et al. Transmission of SARS-CoV-2 on mink farms between humans and mink and back to humans. Science 2021;371(6525):172 – 7. http://dx.doi.org/10.1126/science.abe5901.
12. Chandler JC, Bevins SN, Ellis JW, Linder TJ, Tell RM, Jenkins-Moore M, et al. SARS-CoV-2 exposure in wild white-tailed deer (*Odocoileus virginianus*). bioRxiv, 2021. http://dx.doi.org/10.1101/2021.07.29.454326.
13. Delahay RJ, de la Fuente J, Smith GC, Sharun K, Snary EL, Girón LF, et al. Assessing the risks of SARS-CoV-2 in wildlife. One Health Outlook 2021;3:7. http://dx.doi.org/10.1186/s42522-021-00039-6.
14. Huang K, Zhang YF, Hui XF, Zhao Y, Gong WX, Wang T, et al. Q493K and Q498H substitutions in spike promote adaptation of SARS-CoV-2 in mice. EBioMedicine 2021;67:103381. http://dx.doi.org/10.1016/j.ebiom.2021.103381.
15. Wang L, Su S, Bi YH, Wong G, Gao GF. Bat-origin coronaviruses expand their host range to pigs. Trends Microbiol 2018;26(6):466 – 70. http://dx.doi.org/10.1016/j.tim.2018.03.001.
16. Bayarri-Olmos R, Rosbjerg A, Johnsen LB, Helgstrand C, Bak-Thomsen T, Garred P, et al. The SARS-CoV-2 Y453F mink variant displays a pronounced increase in ACE-2 affinity but does not challenge antibody neutralization. J Biol Chem 2021;296:100536. http://dx.doi.org/10.1016/j.jbc.2021.100536.

Perspectives

Targeted Prevention and Control of Key Links in Airports to Mitigate Public Health Risks

Dongqun Xu[1,#]; Zhuona Zhang[1]; Qin Wang[1]; Xia Li[1]

Airports are the gateways of foreign trade goods, inbound and outbound people, etc., as well as an important gathering places of domestic long-distance passenger and cargo transportation. On July 20, 2021, 9 positive cases of coronavirus disease 2019 (COVID-19) were found in routine nucleic acid tests of staff in key positions at Nanjing Lukou Airport. Epidemiological investigation and analysis showed that the cabin environment was contaminated with COVID-19 by infected passengers of Russian inbound flight CA910 from Russia on July 10 and led to an infection of a cleaning staff member. The epidemic at Lukou Airport then caused the spread of families, communities, and spillovers to 38 cities in 14 provincial-level administrative divisions (PLADs) in China and became the epidemic with the most widespread and large number of infected people in China since the epidemic in Wuhan. Subsequently, the nucleic acid test of a foreign cargo aircraft service staff member at the Shanghai Pudong Airport cargo area was positive on August 2, 2021, and a new case in Haikou was found in a porter of Haikou Meilan Airport Cargo Company on August 5. Several of the above outbreaks were airport related. The pandemic has brought serious transmission risks and challenges to airports.

CHARACTERISTICS AND RELATED WORK IN THE AIRPORT AREA

In the airport area, there are many onsite units involving different jobs and scenarios where lots of people work or engaged in activities. During the COVID-19 pandemic, additional work of epidemic prevention, control, and disposal has been increased. The following takes inbound passenger and cargo flights as an example to introduce the related working process.

The inbound passengers need to go through immigration formalities by the customs and border inspection, take temperature measurements, health declaration verification, epidemiological investigation, collect swab samples for nucleic acid testing before picking up their baggage. Then all are sent to designated isolation hotels by special transfer vehicles. The aircraft need to be cleaned and disinfected after all personnel have disembarked and unloaded their luggage. Space, passage, and articles touched by passengers, as well as special vehicles after completing the transferring and returning, need to be terminally disinfected.

After the arrival of the inbound cargo flight, both cold chain goods and ordinary goods need to be subject to health quarantine by the customs department. Then, relevant personnel shall unload the goods from the aircraft, spray and disinfect the outer surface, transfer them to the fixed tally area of the cargo station by pallet truck, and transport them to the designated area or warehouse for storage after tally. Cold chain goods shall be stored at different temperatures. The goods can be delivered after customs declaration and clearance.

PUBLIC HEALTH RISKS ASSOCIATED WITH AIRPORTS

In view of the serious situation of COVID-19 in the world, it is necessary to sort out the risk and management loopholes related to air passenger and cargo transportation according to the characteristics and related work in airport area, as well as previous epidemic transmission events related to the airports.

Transmission Risks Involving Inbound Passengers

Previously, only aisle, catering counters, and toilets were disinfected for inbound flights, but all areas may be contaminated due to being touched and moved by symptomatic or asymptomatic infected persons. In addition, disinfection techniques were not standardized. For example, cleaning and waste removal personnel did not wear personal protective equipment in strict accordance with protective requirements, resulting in infection. If closed-loop management is not implemented for these personnel, the infection will continue to spread and spillover like Nanjing Lukou Airport. Usually, new arrivals will stay at the airport for up to 4–8 hours. During this period, the passengers are in relatively close proximity. They do not wear masks, drink, or eat freely, while the supply and return air of the central air conditioning system in the terminal area is turned on, resulting in the risk of droplets, fomite, and even long-distance aerosol transmission. The World Health Organization (WHO) and the US CDC officially acknowledged inhalation of virus-laden aerosols as the main mode in spreading severe acute respiratory syndrome coronavirus 2 (SARS-CoV-2), the virus that causes COVID-19, at both short and long ranges (*1–2*). The Supplementary Materials (available in http://weekly.chinacdc.cn/) provide the evidence that we carried out field simulation experiments in Shenzhen Baoan Airport. It showed that aerosols could spread over a long distance through the supply and return air of the central air conditioning system. It should also be noted here that although some airports physically isolate the activity area of inbound personnel from the activity area of domestic passengers through partition, if the return air of central air conditioning is right into the activity area of inbound personnel and the same unit supplies air to the domestic area or airport transportation hub through pipeline, the risk of aerosol transmission needs to be further assessed. All items or facilities touched or used by infected cases, such as elevator buttons, seat armrests, and toilets can be contaminated. It has been reported that SARS-CoV-2 can be detected in feces and urine (*3–6*). During toilet flushing, a large number of virus aerosol particles are generated, contaminating the environment around the squatting or sitting toilet (*7–8*). There is the risk of exposure to fomite and aerosol transmission.

Transmission Risks Associated with Imported Goods

Under specific conditions, such as low temperatures, the virus can survive on the surface of imported goods, and the goods are only the load medium of the virus, the contamination of imported goods may be caused by infected personnel. When a cluster epidemic breaks out in seafood or meat processing enterprises, infected stuff will contaminate cold chain foods during food processing (*9–10*). The workers unloading cold chain goods from the aircraft will be at risk of infection if they do not wear personal protective equipment in strict accordance with the protection requirements. Although the outer package surface is supposed to be sprayed for disinfection after the goods unloading from the aircraft, the disinfection methods are not standardized, especially for cold chain goods, and without using low temperature disinfection technology. When the disinfecting unqualified goods are subsequently transported to the fixed tally area, they will contaminate the pallet truck and cause personnel infection in the process of tally. If closed-loop management is not implemented for the foreign cargo aircraft service personnel, freight company porters, special vehicle drivers, tally clerks, and other relevant personnel in the airport freight, the infection will continue to spread and spillover. In addition, if the small package is contaminated, it will also cause the infection risk of contact personnel such as opening the outer package for warehousing and subsequent sales links.

RECOMMENDATIONS TO REDUCE THE RISK OF COVID-19 TRANSMISSION AND SPREAD AT AIRPORTS

In order to reduce the risk of COVID-19 transmission and spread through aviation channels, the following recommendations are made.

Prevention and Control Measures for International Passenger Flights

The working and personnel activity areas of international (regional) flights and domestic flights should be separated, and it is best to use an independent terminal. The targeted prevention and control measures should be implemented by comprehensive analysis of the epidemic situation, flight range, and passenger occupancy rate at the flight origin. Flights involving epidemic diseases shall park at remote locations. The inbound passengers should use special channels of corridor bridges, customs, border inspection, baggage turntables, and customs baggage inspection. The stay time of inbound personnel in the airport area after arrival should be shortened, and they need to be transferred to the designated hotel by special vehicles as soon as possible. The personnel for disinfection, cleaning, and garbage removal of international flights should be fixed, and they should take good personal protection when performing operations. These personnel should implement closed-loop management, centralized living, fixed rest areas, fixed vehicles and equipment they use, and prompt reports on any health abnormalities (*11*). Terminal disinfection should be carried out on high-risk flights and flights of persons with fever and/or respiratory symptoms, suspected cases, confirmed cases, and asymptomatic infected persons, including all potentially contaminated environments, surfaces, waste, and air, etc. The service organization implementing terminal disinfection should obtain corresponding qualifications. Irrelevant personnel are strictly prohibited to get on and off the aircraft. The crew will be transferred to the designated hotel by closed-loop management. Special vehicles to complete the delivery mission should be disinfected. Quarantine areas, toilets, checked baggage, baggage carousels, and passenger trolleys for inbound passengers should be disinfected every 2–4 hours according to the passenger flow. Flights with abnormal passengers and key tasks should be disinfected at any time. The central air conditioning system in terminal areas should be cleaned and disinfected regularly.

Prevention and Control Measures for International Cargo Flights

The areas for international (regional) cargo flights should be separated. The targeted prevention and control measures should be implemented by comprehensively analyzing the cargo types, epidemic situation at the place of origin, air temperature at the place of origin/arrival, etc. The imported goods operators should implement closed-loop management, centralized residence, fixed personnel, fixed site, fixed equipment and fixed rest areas, fixed vehicles and equipment they use, and timely reporting of any health abnormalities. They should take good personal protection when handling cargo on board. Aircraft and unloaded goods should be subject to preventive disinfection, and cold chain goods should use low-temperature disinfection technology. If the airport of origin can provide proof that the cargo and container have been effectively disinfected before flight departure, the airport of destination may no longer disinfect again. Aviation plates, boxes, net covers, straps, and other containers and their accessories must be fully disinfected after the import cargo operation is completed. Forklifts, tractors, and pallets for transporting goods should be disinfected at least once a day. Operation equipment for imported cold chain goods must be dedicated and disinfected every four hours. The working area and staff rest room should be disinfected at least every four hours. The disinfection interval for toilets should be increased according to the use. The materials and garbage produced in the high-risk link of import goods operation should undergo centralized disinfection and disposed properly.

In conclusion, the Chinese requirements for normalized epidemic prevention and control of "timely detection, rapid disposal, and precise control" for the prevention and control of the epidemic can be fulfilled by formulating and implementing full-process and full-link prevention and control measures in the airport area, strengthening personal protection and disinfection.

Funding: Supported by the Key Program of National Natural Science Foundation of China (Grant No. 92043201).

doi: 10.46234/ccdcw2021.212

Corresponding author: Dongqun Xu, xudq@chinacdc.cn.

[1] China CDC Key Laboratory of Environment and Population Health, National Institute of Environmental Health, Chinese Center for Disease Control and Prevention, Beijing, China.

Submitted: September 19, 2021; Accepted: October 01, 2021

REFERENCES

1. World Health Organization. Coronavirus disease (COVID-19): how is it transmitted? 2020. https://www.who.int/news-room/q-a-detail/coronavirus-disease-covid-19-how-is-it-transmitted. [2021-9-19].
2. U. S. Centers for Disease Control and Prevention. Scientific brief: SARS-CoV-2 transmission. 2021. https://www.cdc.gov/coronavirus/2019-ncov/science/science-briefs/sars-cov-2-transmission.html. [2021-9-19].
3. Holshue ML, DeBolt C, Lindquist S, Lofy KH, Wiesman J, Bruce H, et al. First case of 2019 novel coronavirus in the United States. N Engl J Med 2020;382(10):929 – 36. http://dx.doi.org/10.1056/NEJMoa2001191.
4. Xie CB, Jiang LX, Huang G, Pu H, Gong B, Lin H, et al. Comparison of different samples for 2019 novel coronavirus detection by nucleic acid amplification tests. Int J Infect Dis 2020;93:264 – 7. http://dx.doi.org/10.1016/j.ijid.2020.02.050.
5. Wölfel R, Corman VM, Guggemos W, Seilmaier M, Zange S, Müller MA, et al. Virological assessment of hospitalized patients with COVID-2019. Nature 2020;581(7809):465 – 9. http://dx.doi.org/10.1038/s41586-020-2196-x.
6. Jeong HW, Kim SM, Kim HS, Kim YI, Kim JH, Cho JY, et al. Viable SARS-CoV-2 in various specimens from COVID-19 patients. Clin Microbiol Infect 2020;26(11):1520 – 4. http://dx.doi.org/10.1016/j.cmi.2020.07.020.
7. Li YY, Wang JX, Chen X. Can a toilet promote virus transmission? From a fluid dynamics perspective. Phys Fluids 2020;32(6):065107. http://dx.doi.org/10.1063/5.0013318.

8. Li X, Wang Q, Ding P, Cha YE, Mao YX, Ding C, et al. Risk factors and on-site simulation of environmental transmission of SARS-CoV-2 in the largest wholesale market of Beijing, China. Sci Total Environ 2021;778:146040. http://dx.doi.org/10.1016/j.scitotenv.2021.146040.
9. Nat Herz. COVID-19 outbreak in pacific northwest seafood industry as season ramps up. 2020. https://www.npr.org/sections/coronavirus-live-updates/2020/06/05/870312092/pacific-northwest-seafood-industry-faces-covid-19-outbreak-as-season-ramps-up. [2021-9-19].
10. Dyal JW, Grant MP, Broadwater K, Bjork A, Waltenburg MA, Gibbins JD, et al. COVID-19 among workers in meat and poultry processing facilities–19 states, April 2020. MMWR Morb Mortal Wkly Rep 2020;69(18):557 – 61. http://dx.doi.org/10.15585/mmwr.mm6918e3.
11. The State Council's Joint Prevention and Control Mechanisms for the Response to COVID-19. Notice on issuing the disinfection work plan for inbound passenger aircraft. Joint Prevention and Control Mechanism Zongfa 2021(100):2021.

Supplementary Material

On June 14, 2021, a customs officer who engaged in an epidemiological investigation at Shenzhen Bao'an Airport was confirmed to be infected with severe acute respiratory syndrome coronavirus 2 (SARS-CoV-2) at the fever clinic. He participated in the epidemiologic investigation of passengers on Flight CA868 from South Africa on June 10. In order to investigate whether inhaling virus-laden aerosols is a mode of long-distance transmission of COVID-19, we conducted a field aerosol simulation experiment at the inbound passenger waiting and epidemiological investigation area of Shenzhen Bao'an Airport. The same air conditioning unit is used for air supply and return in this area. Multiple air supply outlets were located in the waiting area and the epidemiological investigation area, and multiple air return outlets were located in the front and back of the epidemiological investigation area. The inbound passengers in the waiting area were relatively dense and did not wear masks sometimes.

We used fluorescent polystyrene microspheres consistent with the similar aerodynamic characteristics of the SARS-CoV-2 spike pseudovirus to simulate respiration for 2 hours in the waiting area (the specific methods were described as previously published paper) (*1*). Samples of sedimentation on the air supply and return outlets were collected with cotton swabs and the concentration of aerosol particles with different sizes were monitored in the epidemiological investigation area about 25 meters away from the waiting area. It was found that after 20 minutes of fluorescent microspheres were aerosolized, the number concentration of aerosol particles with different sizes in the epidemiological investigation area increased significantly. The fluorescent microspheres were detected at the air supply and return outlets after 2 hours. The results were shown in Supplementary Figure S1. It showed that the simulated viral aerosol can spread from the waiting area to the epidemiological investigation area through the air supply and return of the central air-conditioning system and can spread over a long distance.

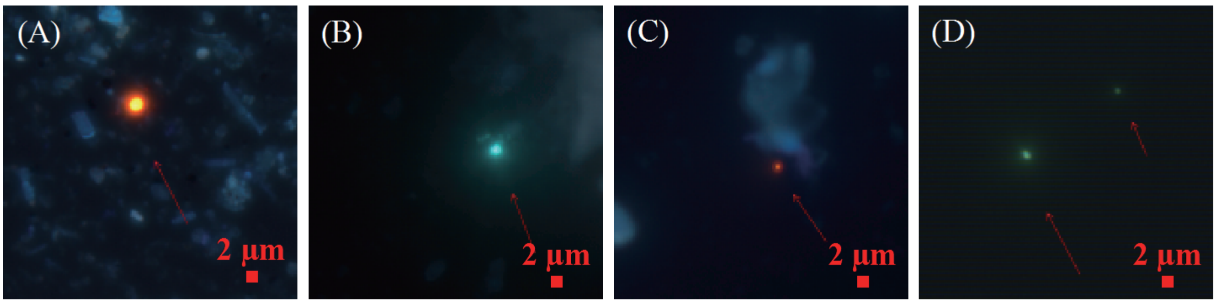

SUPPLEMENTARY FIGURE S1. Field aerosol simulation experiment results at the inbound passenger waiting and epidemiological investigation area of Shenzhen Bao'an Airport. Representative photos of fluorescent microspheres (yellow and green) of air samples using natural sedimentation on (A) air return outlet of the front of epidemiological investigation area; (B) air return outlet of the back of epidemiological investigation area; (C) air supply outlet of the front of epidemiological investigation area; (D) air supply outlet of the waiting area.

REFERENCES

1. Zhang ZN, Li X, Wang Q, Xu J, Jiang QQ, Jiang SL, et al. Field simulation of aerosol transmission of SARS-CoV-2 in a special building layout-Guangdong province, China, 2021. China CDC Wkly 2021;3(34):711 – 5. http://dx.doi.org/10.46234/ccdcw2021.176.

Outbreak Reports

Eleven COVID-19 Outbreaks with Local Transmissions Caused by the Imported SARS-CoV-2 Delta VOC — China, July–August, 2021

Lei Zhou[1]; Kai Nie[2]; Hongting Zhao[3]; Xiang Zhao[2]; Bixiong Ye[4]; Ji Wang[2]; Cao Chen[2]; Hong Wang[2]; Jiangli Di[5]; Jinsong Li[2]; Chao Li[1]; Zhixiao Chen[2]; Ruiqi Ren[1]; Peihua Niu[2]; Hui Chen[6]; Tao Chen[2]; Yali Wang[1]; Lili Li[2]; Bingxue Han[7]; Ruhan A[2]; Si Chen[7]; Dan Li[1]; Dan Li[3]; Chunxia Jin[8]; Xin Zhang[9]; Jiangmei Liu[10]; Chunyu Xu[4]; Yecheng Yao[11]; Yenan Feng[2]; Zhili Li[3]; Bike Zhang[12]; Yang Song[2]; Peter Hao[12]; Yanping Zhang[1]; Hao Li[12]; Qun Li[1]; George F. Gao[12]; Guoqing Shi[1,#]; Wenbo Xu[2,#]

Starting from December 2019, Wuhan, China, encountered the first outbreak of coronavirus disease 2019 (COVID-19) (*1–2*). The epidemic was successfully suppressed by strict containment so that the number of infected people was reduced to 0 on April 8, 2020 (*3–4*). After that, China experienced roughly 3 dozen outbreaks with local transmission caused by imported severe acute respiratory syndrome coronavirus 2 (SARS-CoV-2). These outbreaks were then contained by an effective suppression strategy, and the number of infected people has successfully reached zero again. However, local outbreaks of COVID-19 have reappeared in several areas in China recently and were caused by the SARS-CoV-2 Delta variant of concern (VOC) (*5*).

As of August 26, 2021, a total of 1,390 cases of COVID-19 had been reported in 50 cities in 19 provincial-level administrative divisions (PLADs) (Figure 1), all of which were found to involve the Delta variant.

Furthermore, these cases were found to stem from 12 genetically distinct Delta variant imported sources that were grouped into 11 related outbreaks or sporadic case incidents, resulting in 10 geographically separated epidemics including the following areas (Figure 1): Nanjing City of Jiangsu Province; Zhengzhou City of Henan Province; Xiamen City of Fujian Province; Wuxi City of Jiangsu Province; Dehong City of Yunnan Province; Pudong District of Shanghai Municipality; Songjiang District of Shanghai Municipality; Haikou City of Hainan Province; Ningbo City of Zhejiang Province; and Bortala Prefecture of Xinjiang Uygur Autonomous Region.

Starting from July 20, 2021, the number of daily reported infections increased gradually but reached a peak reporting period from July 31 to August 11, 2021. During this peak period, the number of everyday reported cases exceeded 50, and a total of 969 cases were reported during this period, which comprised 69.7% of all cases reported during this series of epidemics. After August 12, the number of daily reported cases decreased significantly.

INVESTIGATION AND RESULTS

The spatial distribution of the cases was shown in Figure 1. The 5 areas with the highest cumulative reported cases were as follows: Yangzhou City of Jiangsu Province (570 cases, 41.0%), Nanjing City of Jiangsu Province (235 cases, 16.9%), Zhengzhou City of Henan Province (139, 10.0%), Wuhan City of Hubei Province (88 cases, 6.3%), and Zhangjiajie City of Hunan Province (76 cases, 5.5%). There were 1,390 cases reported in total, 108 (7.8%) were asymptomatic cases and 1,282 (92.2%) were confirmed symptomatic infections; 660 (47.5%) cases occurred in males; and the median age of the patients was 44 years (interquartile range: 29–58). Populations of all age groups were affected, with most cases occurring in patients aged 20–70 years old. The median age of confirmed and symptomatic infections (45 years) and asymptomatic infections (32 years) differed significantly ($P<0.05$). The occupational categories that comprised the highest proportions and exceeded 10% of the total were as follows: homemakers and unemployed persons (16.0%), retired persons (13.3%), laborers (13.3%), farmers (11.1%), public venue attendants (10.8%), and students (10.2%). More data were available in Table 1.

Nanjing City Epidemic

Of this series of epidemics, the epidemic in Nanjing City affected the largest geographical area and had the most significant cumulative number of cases. The investigation revealed that the index case, which was

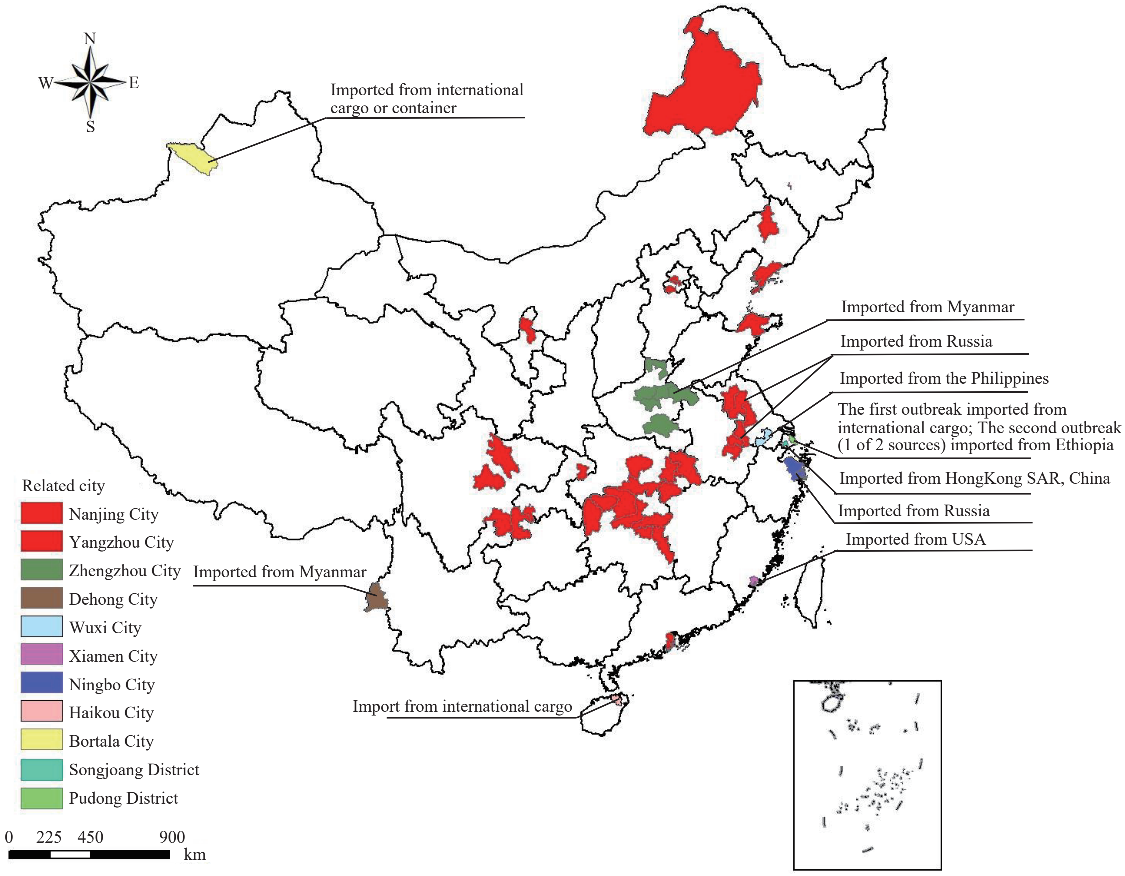

FIGURE 1. Spatial distribution of reported cases in the series of COVID-19 epidemics caused by the Delta variant in China from July 20 to August 26, 2021.

reported on July 20, 2021 most likely happened in a cabin cleaning staff member servicing Air China Flight CA910 from Moscow Sheremetyevo International Airport (SVO) to Nanjing Lukou Airport (NKG) on July 10. The genome of the strain of Delta VOC detected in the index case was identical to the genome of the strain isolated from an imported patient found in a passenger of the flight, who was tested while in mandatory two-week quarantine. Furthermore, this identical strain was detected in several other local cases in Nanjing in the days after the index case was found.

After the virus was introduced to airport staff through the cleaning staff member, it most likely first spread to other cleaning staff members and then to airport passengers, local communities, and families. This resulted in further community transmission, eventually spilling over to other cities and provinces.

From July 20 to 29, 2021, the reported infections in this epidemic were mostly limited to Nanjing. However, starting on July 30, the proportion of reported infections in neighboring Yangzhou City gradually exceeded that of Nanjing. As of August 26, 2021, this epidemic resulted in a total of 1,162 reported infections across 38 cities in 14 PLADs. The 5 areas with the highest number of reported illnesses were as follows: Yangzhou City (570 cases), Nanjing City (235 cases), Wuhan City (88 cases), Zhangjiajie City (76 cases), and Jingmen City (58 cases). Nanjing Lukou Airport was fully closed for prevention and control measures starting on July 26.

Zhengzhou City Epidemic

The first reported cases of the Zhengzhou City epidemic occurred in a pregnant woman and a cleaning staff member in the Sixth People's Hospital of Zhengzhou. After the cases were reported on July 31, all hospital-related personnel, including staff members, patients, and accompanying persons, immediately underwent nucleic acid testing, which yielded a total of 32 infection cases that were found that day. The index case was most likely in an accompanying person visiting a patient in the Tuberculosis (TB)

TABLE 1. Demographic data for the series of COVID-19 epidemics caused by the B.1.617.2 (Delta) variant in China from July 20 to August 26, 2021

Characteristics	Total, n (%)	Asymptomatic infections, n (%)	Confirmed, symptomatic infections, n (%)	*P*-value
Sex				
Male	67 (10.2)	660 (47.5)	593 (89.8)	<0.05
Female	41 (5.6)	730 (52.5)	689 (94.4)	
Age				
Mean ± standard deviation	32.0 ± 17.8	43.1 ± 20.8	44.1 ± 20.7	<0.05
Median (interquartile range)	32 (17–46)	44 (29–58)	45 (30–59)	
Range (minimum–maximum)	1–77	0–91	0–91	
<18 years old	28 (14.4)	194 (14.0)	166 (85.6)	<0.05
18–59 years old	75 (8.6)	873 (62.8)	798 (91.4)	
≥60 years old	5 (1.5)	323 (23.2)	318 (98.5)	
Occupation				
Homemakers and unemployed persons	9 (4)	223 (16.0)	214 (96)	<0.05
Retirees	2 (1.1)	185 (13.3)	183 (98.9)	
Worker	28 (15.1)	185 (13.3)	157 (84.9)	
Farmer	5 (3.2)	154 (11.1)	149 (96.8)	
Public venue attendant	9 (6)	150 (10.8)	141 (94)	
Student	23 (16.2)	142 (10.2)	119 (83.8)	
Public staff	7 (10)	70 (5.0)	63 (90)	
Toddler/child	7 (12.1)	58 (4.2)	51 (87.9)	
Sanitation staff	1 (1.9)	53 (3.8)	52 (98.1)	
Medical staff	3 (8.1)	37 (2.7)	34 (91.9)	
Catering industry	1 (5.9)	17 (1.2)	16 (94.1)	
Teacher	3 (17.6)	17 (1.2)	14 (82.4)	
Driver	0 (0)	11 (0.8)	11 (100)	
Other	10 (11.4)	88 (6.3)	78 (88.6)	
Epidemic center				
Nanjing, Jiangsu	101 (8.7)	1,162 (83.6)	1,061 (91.3)	<0.05
Zhengzhou, Henan	1 (0.6)	167 (12.0)	166 (99.4)	
9 other outbreaks	6 (9.8)	61 (4.4)	55 (90.2)	
Total	108 (7.8)	1,390 (100)	1,282 (92.2)	

Complications Department of the Sixth People's Hospital of Zhengzhou; this accompanying person started experiencing symptoms on July 24.

Previously, the Sixth People's Hospital of Zhengzhou admitted two imported cases of COVID-19 from the Yangon City of Myanmar. The cases occurred in persons entering China in early July and were admitted to the hospital for isolation treatment. Since the isolation ward for COVID-19 at the hospital was adjacent to TB ward, the transmission was suspected to occur that first infected attendants and patients of the department, then spread through the rest of the hospital through close contact with other medical staff, cleaning staff, accompanying persons, and other populations. Afterward, COVID-19 likely spilled out to the rest of Zhengzhou and 5 other cities in Henan Province.

As of August 26, a total of 167 cases have been linked to this epidemic that stemmed from the Sixth People's Hospital of Zhengzhou. The genetic sequence of the first reported case, the likely index case, and the imported cases from Myanmar were homologous (Figure 2), so the imported cases were the possible source of this epidemic. The Sixth People's Hospital of

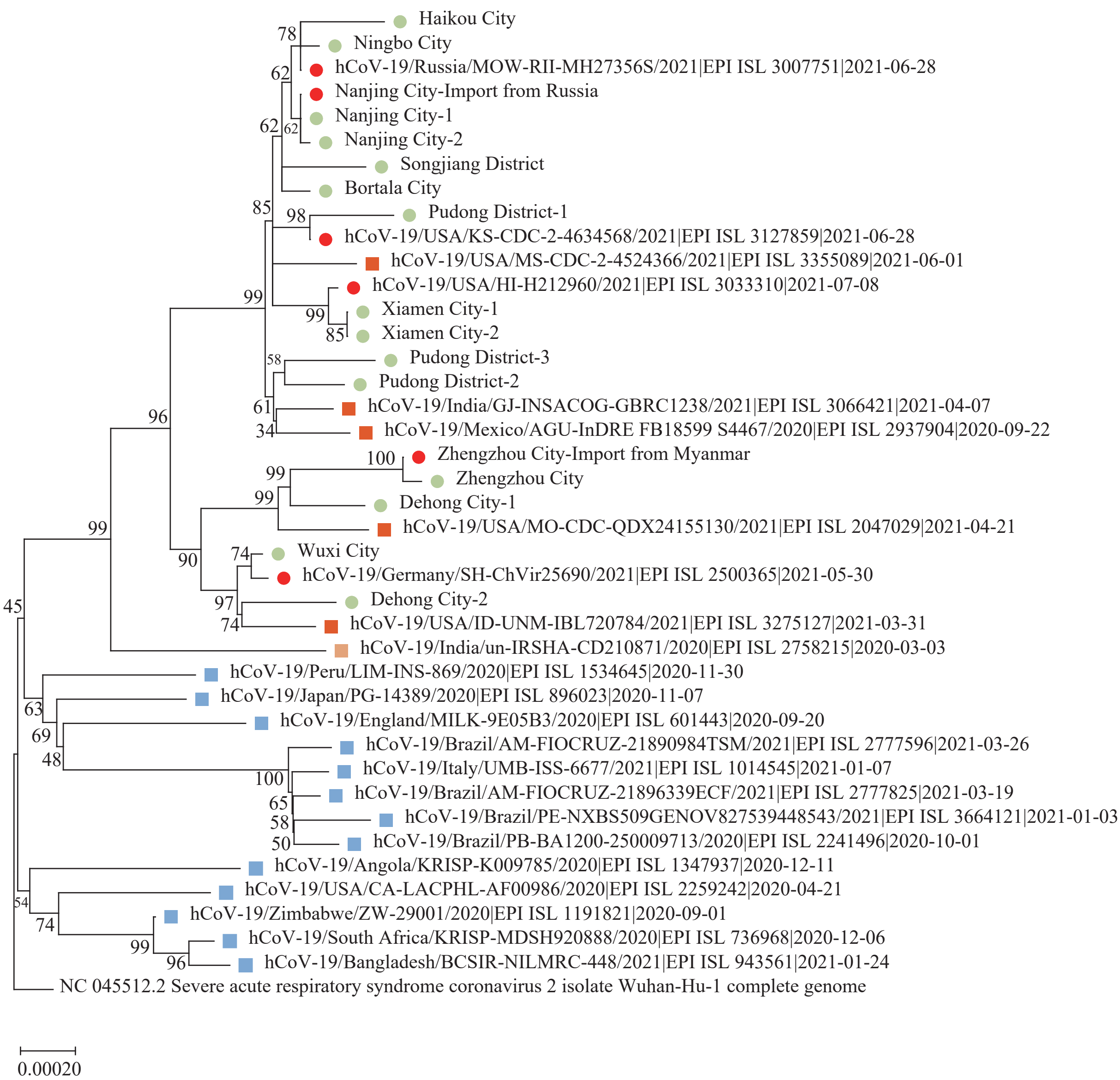

FIGURE 2. Phylogenetic analysis of SARS-CoV-2 based on full-length genome sequences.
Note: The Delta variants that caused the eleven recent outbreaks in China are indicated by green dots, and the Delta variants of imported case (or GISAID) with the highest genome homology to the local epidemic strains, the Delta variants from outside China (including lineages B.1.617.2, AY.1, AY.2, AY.3, and AY.3.1), the Kappa variants (lineage B.1.617.1), and the other VOCs and VOIs are indicated by red dots, orange squares, light orange square, and blue squares, respectively. The tree was rooted using the prototype strain isolated in Wuhan. A neighbour-joining phylogenetic tree was constructed using MEGA (v7.0), and the Kimura 2-parameter model with 1,000 bootstrap replicates was used.

Zhengzhou and its neighboring communities were closed for prevention and control measures starting on July 31.

Other Epidemics

Since July 20, 2021, 9 other smaller-scale epidemics/outbreaks have been reported and investigated in other parts of the country; all 9 outbreaks were suspected originated from imported cases or cargos contaminated by SARS-CoV-2. As of August 26, a total of 61 cases had been reported in the following areas: Dehong City of Yunnan Province (40 cases); Xiamen City of Fujian Province (5 cases); Wuxi City of Jiangsu Province (1 case); Pudong District of Shanghai Municipality (8 cases, from three independent sources); Songjiang District of Shanghai Municipality (2 cases); Haikou City of Hainan Province (1 case); Ningbo City of Zhejiang Province (1 case); and Bortala Prefecture of Xinjiang Uygur Autonomous Region (3 cases).

The resulting investigation yielded a variety of causes. The Dehong Epidemic was most likely due to imported cases in individuals entering China through the land border with Myanmar. The Xiamen Outbreak was most likely caused by pilots of international cargo flights from the United States. The source of the Delta variant in the sporadic cases incidents in Wuxi and Songjiang District were related to imported cases in local designated hospitals. The source of the first outbreak in Pudong was most likely due to a ground crewmember of Pudong Airport shuttle crews for international flights. The source of the sporadic cases in Haikou and Ningbo and the second outbreak in Pudong were most likely to be spread by international cargo porters in the airports of or ports the three cities. The Bortala Prefecture Outbreak was probably due to transmission by international cargo or container. Genetic sequencing (Figure 2), molecular epidemiological analysis, and epidemiological methods indicated the source of the Delta variant of the 7 COVID-19 epidemics/outbreaks were linked to the following countries/areas: the Dehong outbreak was related to imported cases from Myanmar; the Nanjing outbreak from Russia; the Wuxi outbreak from the Philippines; the Zhengzhou outbreak from Myanmar; the Xiamen outbreak from the United States; the Ningbo outbreak from Russia; and the second Pudong District outbreak (one of the two sources) from Ethiopia; the Songjiang District outbreak from HongKong SAR, China. No highly homologous genome sequences were found of the other three outbreaks related to the Delta variant (Xinjiang, Haikou, and one of the two Pudong oubreaks in Shanghai) among the SARS-CoV-2 database of domestic and on Global Initiative on Sharing Avian Influenza Data-EpiCoV (GISAID-EpiCoV) platform (https://www.gisaid.org). The detected strains circulated in different periods but were closely related.

PUBLIC HEALTH RESPONSE

Following the emergence of the epidemics, provincial authorities initiated an emergency response, and the National Health Commission (NHC) immediately formed a working group that included experts from China CDC and delegated them to Nanjing, Zhangjiajie, Yangzhou, Zhengzhou, Wuhan, and other affected areas to provide onsite guidance. Several affected venues, including Nanjing Lukou Airport and the Sixth People's Hospital of Zhengzhou, were closed to respond to the epidemic and reduce transmission through prevention and control measures.

Prevention and control of these epidemics were still based on the previous strategies and measures (*6*). Risk areas were delineated, at-risk people and close contacts were determined and tracked, large-scale population nucleic acid screening was implemented, and detection and management of the sources of infection were completed as early as possible. Responsible societal stakeholders were mobilized to encourage compliance and cooperation by fully utilizing existing community-led grassroots grid management systems.

DISCUSSION

The sources of SARS-CoV-2 infections for several epidemics inside China after the wave of Wuhan outbreak have been found previously. For instance, imported cases and related transmission were caused by flights (*7*), carried by crewmembers (*8*), carried by community members (*9*), and spread in hospital settings (*10*). Increasing awareness and remaining vigilant will help prepare the necessary emergency response resources and prevent the uncontrolled spread of COVID-19.

The measures utilized in these responses and other strategies helped terminate community transmission, strengthen infection control, and prevented spread in critical venues such as medical institutions, designated patient isolation facilities, and nursing homes. As is known, the transmission of Delta variant was even faster and more severe than the prototype strain that was isolated in Wuhan (*5*); in order to ensure the suppression of this virus, the time period for considering a contact to be a close contact was lengthened to increase the sensitivity of close contact identification to find infected individuals. Furthermore, the timely release of information and communication of risks allowed for heightened public awareness and, when coupled with improved health education for the public, helped achieve better use of emergency response resources and better outcomes for the epidemic prevention and control strategies. Through careful implementation of various active and effective measures, the number of cases in this series of epidemics has been reduced to zero.

Funding: Supported by the National Natural Science Foundation (grant number 71934002) of the People's Republic of China.

doi: 10.46234/ccdcw2021.213

[#] Corresponding authors: Wenbo Xu, xuwb@ivdc.chinacdc.cn; Guoqing Shi, shigq@chinacdc.cn.

[1] Public Health Emergency Center, Chinese Center for Disease Control and Prevention, Beijing, China; [2] NHC key laboratory for Medical Virology, National Institute for Viral Disease Control and Prevention, Chinese Center for Disease Control and Prevention, Beijing, China; [3] Division of Infectious Disease, Key Laboratory of Infectious Disease Surveillance and Ear-warning, Chinese Center for Disease Control and Prevention, Beijing, China; [4] National Institute of Environmental Health, Chinese Center for Disease Control and Prevention, Beijing, China; [5] National Center for Women and Children's Health, Chinese Center for Disease Control and Prevention, Beijing, China; [6] National Center for Tuberculosis Control and Prevention, Chinese Center for Disease Control and Prevention, Beijing, China; [7] Weifang Medical University, Weifang, Shandong, China; [8] Anti-plague Institute of Hebei Province, Zhangjiakou, Hebei, China; [9] The First Institue for Endemic Diseases Control and Prevention of Jilin Province, Baicheng, Jilin, China; [10] National Center for Chronic and Noncommunicable Disease Control and Prevention, Chinese Center for Disease Control and Prevention, Beijing, China; [11] National Institute for Nutrition and Health, Chinese Center for Disease Control and Prevention, Beijing, China; [12] Chinese Center for Disease Control and Prevention, Beijing, China.

Submitted: September 23, 2021; Accepted: October 01, 2021

REFERENCES

1. Tan WJ, Zhao X, Ma XJ, Wang WL, Niu PH, Xu WB, et al. A Novel coronavirus genome identified in a cluster of pneumonia cases—Wuhan, China 2019–2020. China CDC Wkly 2020;2(4):61 – 2. http://dx.doi.org/10.46234/ccdcw2020.017.
2. Zhu N, Zhang DY, Wang WL, Li XW, Yang B, Song JD, et al. A novel coronavirus from patients with pneumonia in China, 2019. N Engl J Med 2020;382(8):727 – 33. http://dx.doi.org/10.1056/NEJMoa2001017.
3. Li ZJ, Chen QL, Feng LZ, Rodewald L, Xia YY, Yu HL, et al. Active case finding with case management: the key to tackling the COVID-19 pandemic. Lancet 2020;396(10243):63 – 70. http://dx.doi.org/10.1016/S0140-6736(20)31278-2.
4. Zhou L, Wu ZY, Li ZJ, Zhang YP, McGoogan JM, Li Q, et al. One hundred days of coronavirus disease 2019 prevention and control in China. Clin Infect Dis 2021;72(2):332 – 9. http://dx.doi.org/10.1093/cid/ciaa725.
5. Zhang M, Xiao JP, Deng AP, Zhang YT, Zhuang YL, Hu T, et al. Transmission dynamics of an outbreak of the COVID-19 delta variant B. 1. 617. 2—Guangdong Province, China, May–June. China CDC Wkly 2021(27):584 – 6. http://dx.doi.org/10.46234/ccdcw2021.148.
6. Liu FF, Zheng CJ, Wang LP, Geng MJ, Chen H, Zhou S, et al. Interpretation of the protocol for prevention and control of COVID-19 in China (Edition 8). China CDC Wkly 2021;3(25):527 – 30. http://dx.doi.org/10.46234/ccdcw2021.138.
7. Cheng C, Wang L, Lyu ZQ, Peng B, Li YH, Kong DF, et al. Four COVID-19 cases of new variant B. 1. 351 first emerging in South Africa in Chinese passengers on same flight — Shenzhen, China, January. China CDC Wkly 2021(8):175 – 7. http://dx.doi.org/10.46234/ccdcw2021.049.
8. Chen FJ, Li BS, Hao P, Song Y, Xu WB, Liu NK, et al. A case of new variant COVID-19 first emerging in South Africa detected in airplane pilot — Guangdong Province, China, January 6, 2021. China CDC Wkly 2021;3(2):28 – 9. http://dx.doi.org/10.46234/ccdcw2021.007.
9. Qi SX, Zhao X, Hao P, Liu NK, Gao GF, Song Y, et al. Two reemergent cases of COVID-19 — Hebei Province, China, January 2, 2021. China CDC Wkly 2021;3(2):25 – 7. http://dx.doi.org/10.46234/ccdcw2021.006.
10. Xin HL, Liang JW, Jiang FC. A hospital superspreading event of COVID-19 — Qingdao City, Shandong Province, China, 2020. China CDC Wkly 2020;2(34):655 – 7. http://dx.doi.org/10.46234/ccdcw2020.162.

Methods and Applications

Braking Force Model on Virus Transmission to Evaluate Interventions Including the Administration of COVID-19 Vaccines — Worldwide, 2019–2021

Shengyi Zhong[1,&]; Zhe Chen[2,&]; Yun Wang[3]; Pucong Sheng[1]; Shuxin Shi[1]; Yongxi Lyu[1]; Ruobing Bai[1]; Pengyu Wang[1]; Jiangjing Dong[1]; Jianbo Ba[4]; Xinmiao Qu[5]; Jian Lu[6,7,#]

ABSTRACT

Introduction: Assessing the effects of non-pharmaceutical interventions (NPIs) and vaccines on controlling the coronavirus disease 2019 (COVID-19) is key for each government to optimize the anti-contagion policy according to their situation.

Methods: We proposed the Braking Force Model on Virus Transmission to evaluate the validity and efficiency of NPIs and vaccines. This model classified the NPIs and the administration of vaccines at different effectiveness levels and forecasted the duration required to control the pandemic, providing an indication of the future trends of the pandemic wave.

Results: This model was applied to study the effectiveness of the most commonly used NPIs according to the historic pandemic waves in different countries and regions. It was found that when facing an outbreak, only strict lockdown would give efficient control of the pandemic; the other NPIs were insufficient to promptly and effectively reduce virus transmission. Meanwhile, our results showed that NPIs would likely only slow down the pandemic's progression and maintain a low transmission level but fail to eradicate the disease. Only vaccination would likely have had a better chance of success in ending the pandemic.

Discussion: Based on the Braking Force Model, a pandemic control strategy framework has been devised for policymakers to determine the commencement and duration of appropriate interventions, with the aim of obtaining a balance between public health risk management and economic recovery.

INTRODUCTION

Since the outbreak of coronavirus disease 2019 (COVID-19), caused by severe acute respiratory syndrome coronavirus 2 (SARS-CoV-2) in December 2019, the total number of related deaths worldwide has exceeded 2.8 million (*1*). Every country is currently taking various measures to combat the spread of this disease. However, eradication of this virus or stopping its transmission has been a challenging task. Evidence has shown herd immunity is unlikely to be achieved without intervention or vaccination (*2*–*4*). With the increase of daily new cases (*5*) and the lag in the production of antibodies by the vaccine and their uncertain effectiveness, it is urgent to first control the spread of COVID-19 via non-pharmaceutical interventions (NPIs). NPIs that limit social contact and enable continuance of protective behaviors, such as social distancing, night curfews, mask requirements, and area lockdowns, can help curb the pandemic until vaccines are rolled out (*6*–*9*).

Several countries have experienced three or more waves of the pandemic thus far. In most cases, outbreaks have occurred after the government loosened or withdrew the use of NPIs when the number of infections was lower than a certain threshold. To achieve an optimal balance between public health risks and economic recovery, in addition to the effects of the different NPIs, policymakers must understand the type of NPIs, i.e., mandatory or voluntary compliance, that should be implemented and during which phase of the pandemic these NPIs should be withdrawn.

While vaccines are being rolled out in several countries, it is still crucial to understand the types and timings of the different NPI measures that should be implemented to contain the pandemic effectively. Since the first COVID-19 vaccine was administered in the United Kingdom (UK) in December 2020, followed by numerous countries including the United States (US), Canada, some European countries, and China (*10*), studies on the effect of vaccines at each stage of the shifting population-vaccination ratio are being conducted. Most countries are still far from the goal of having more than 80% of their total population vaccinated. Implementing the most effective and appropriate NPIs during this transition period will help get people's life back to as close to normal as possible.

METHODS

Braking Force Model

A number of epidemiological transmission models have been established to evaluate and predict the increase in the number of COVID-19 cases (*11–18*). Some predictions were made based on the mobility of the virus spread represented by the basic reproduction number, R_0. However, the parameters used in these models were complicated for two reasons. First, there are several unknown aspects of COVID-19, and it remains unclear as to why the virus mutates rapidly. Second, different social and environmental factors, such as government policies, environmental temperature, and population density, had different effects on these parameters. For instance, it would be inappropriate to use the epidemiological parameters of a cold, low-population-density country with good sanitary conditions to forecast the pandemic trajectory in a hotter, high population-density country with minimal government intervention measures.

This study developed a new model, called the Braking Force Model on Virus Transmission to examine and evaluate the validity and efficiency of different anti-contagion policies, including NPIs and vaccines under different situations and conditions and with different sample numbers. Most importantly, the Braking Force Model is not correlated to epidemiological parameters and it extracts information directly from the pandemic data. If we consider the pandemic to be a moving car, SARS-CoV-2 with its high transmissibility can be regarded as stepping on the accelerator, where the speed of spread or transmission of the virus is represented as R_0. The higher the speed, the faster and wider is the spread of the pandemic. Governments brake the car by implementing different NPIs. In other words, whenever governments release the brakes, the car will pick up the speed again. Another way to slow down the car would be to increase the friction between the ground and the wheels of the car by making the ground extremely muddy or bumpy, such that the car stops — in other words, the pandemic stops, which is the desired effect of vaccination and can be achieved by breaking the chain of transmission. This analogy demonstrates that the speed of virus transmission is directly related to the dynamics of virus transmissibility, use of NPIs, and vaccination. These are the key factors determining the shape of the pandemic wave.

The proposed model can be expressed as follows:

$$a_{Covid19} = \mu_{vaccine} \cdot a_{R0} + \sum a_{NPI} \cdot \gamma$$

$a_{Covid19}$=the acceleration of the pandemic at a particular point in time.

a_{R0}=acceleration of the basic reproduction number.

R_0=a variable that depends on the mutation of the virus, temperature, and local population density.

$\mu_{vaccine}$=the coefficient or the vaccination ratio, which is 1 for no antibodies produced by vaccination and 0 when herd immunity is achieved.

a_{NPI}=the acceleration of NPIs. This value is generally negative if it acts as the braking force. The deceleration, which is the absolute value of NPIs from high to low, is in the order of levels A, B, and C. Such a deceleration of the same NPI could vary according to the differences in factors such as anti-contagion policies, local sanitation, and the habits and customs of local people.

γ=coefficient of execution efficiency of the NPIs; a multiplier of a_{NPI}.

To bring down the number of new cases, the absolute value of NPIs and vaccine deceleration must be higher than the basic acceleration of COVID-19. By studying the acceleration $a_{Covid19}$, we can assess the effect of each intervention by profiling the pandemic peak.

At present, policymakers need a model that can be easily adopted to analyze unknown epidemic transmission behaviors by identifying and foreseeing the growth of the pandemic based on the actual circumstances. Drawing from the widely used peak profile method in the field of physics, the Braking Force Model fits the wave without assuming any epidemiological parameters. It is expected that policymakers will be able to refer this model to examine the validity and efficiency of different anti-contagion policies, including the use of NPIs and vaccines to achieve desirable and effective outcomes.

Classification and Forecast

Every increase and subsequent drop in new COVID-19 cases is described as a peak, or a wave. In our study, we extracted information using the peak profile method and determined the pandemic trajectory based on data from the database of new COVID-19 cases in different countries and regions (*10*). We first classified the epidemic control effectiveness manually into three levels. Level A efficiency represented a very efficient control of the pandemic, and the shape of the wave was fairly symmetric. Level B represented a mild control, with a longer tail in the wave shape. Level C represented an unsuccessful control with the number of daily new cases decreasing very slowly with repeated fluctuations (Supplymentary Figure S1, available in http://weekly.chinacdc.cn/).

Our data outlined the interval of the fitting parameters of each level. By using semi-supervised learning, our model can classify the ongoing wave and study the effect of different NPIs as well as vaccines in controlling the pandemic. Using the parameters obtained from peak fitting, our model can also forecast the pandemic tendencies of each ongoing wave under the current anti-contagion policy and provide a prediction parameter $t_{30\%}$ for each wave. This prediction parameter, $t_{30\%}$, represents the time required for the number of new cases to decrease to 30% of the highest number of new cases in a particular wave (see Supplementary Materials "forecast method" for detailed information, available in http://weekly.chinacdc.cn/), which could partially represent the speed of controlling the epidemic. A flow chart of the algorithm is presented in Figure 1. (Detailed information of the model and algorithm in the Supplementary Materials).

Compared to the classic epidemic model, one of the significant characteristics of the Braking Force Model lies in the fact that all the information is drawn directly from the pandemic data, i.e., historical daily new cases. No hypotheses are made on epidemiological transmissions, like the basic reproduction number (R_0), infection rate, or recovery rate, offering novel perspectives to understanding COVID-19.

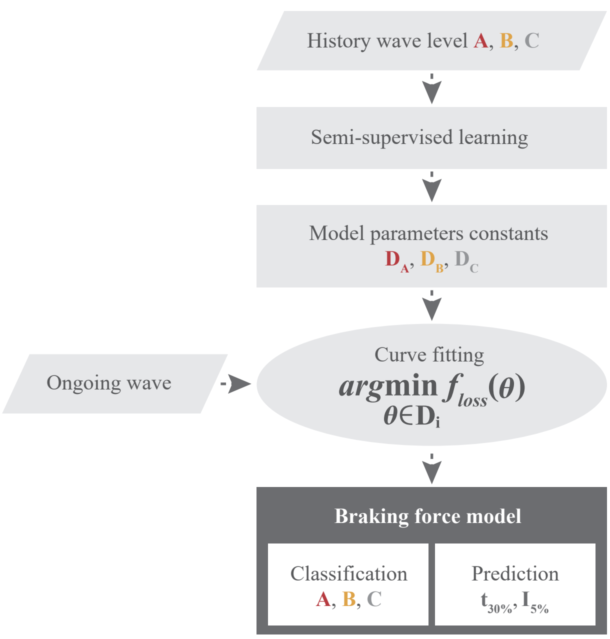

FIGURE 1. Flow chart of the classification and forecast of pandemic waves using the peak profile method.
Note: I%: A parameter to predict the number of new daily cases as a percentage relative to the highest number of daily cases during the current wave of the pandemic.

RESULTS

Braking Force Effects of NPIs

We used the Braking Force Model to further study the effectiveness of the most commonly used NPIs, such as lockdowns, mask-wearing, and social distancing, on controlling the pandemic as well as their optimal implementation periods. Notably, the effectiveness of each NPI can vary according to people's actual behaviors in different countries and during different time periods. The classification is based on the assumption that the interventions are correctly and strictly implemented. Another assumption is that, in most parts of the world, the COVID-19 pandemic was much more severe in the second half of 2020. Hence, we study mainly the history of waves after July 2020 (*1*,*19*), in order to achieve better comparisons between parameters.

Level A Effectiveness — Lockdown

As one of the most severe NPIs, lockdown is usually complemented with other NPIs such as social distancing, night curfews, and mask-wearing. We studied the data of five countries (Supplymenatary Table S1, available in http://weekly.chinacdc.cn/) and classified the effectiveness of lockdown on controlling COVID-19 as Level A, with an average prediction of $t_{30\%}$ of approximately 23 days. Its high effectiveness showed that lockdown is the fastest way to control the outbreak. However, lockdown causes serious societal and economic disruptions, which highlights the importance of finding the optimal duration. Thus, a prediction parameter $I_{5\%}$ was set up for the daily number of new cases being 5% of the highest number of this wave. It is recommended that the lockdown policy should continue until it meets this 5% parameter, i.e., when the current pandemic wave is under control.

Lockdown Example: France

The second round of lockdown in France occurred from October 30 to November 30 of 2020. After two weeks of lockdown, by incorporating the number of new infections on November 10, our Braking Force Model classified this wave as Level A with high efficiency and forecasted that the number of new infections could be reduced to $I_{5\%}$ on December 12. In other words, our model suggested that by December 12, the wave of COVID-19 in France would be under control. It was found that such a forecast had close alignment with reality until the lockdown was lifted on November 30, when the number of new cases were approximately 25% of the peak. Subsequently, the daily new cases bounced back immediately and deviated from our forecast (Figure 2B).

Lockdown Example: Belgium

Belgium had a pandemic wave tendency and anti-contagion policy similar to that of France before the end of November 2020. Belgium had also lifted their lockdown on December 1 at around the same time as France. However, at that time, the number of new cases in Belgium was approximately $I_{15\%}$; the mobility data (Supplymenatary Figure S3, available in http://weekly.chinacdc.cn/) showed that Belgium succeeded to maintain a lower mobility trend than France and the number of new cases continued to decrease to $I_{10\%}$ around the time of Christmas. Despite the gap between reality and our projection of $I_{5\%}$, the pandemic stabilized eventually, as was predicted by our model (Figure 2B).

Level B Effectiveness — Mask-Wearing

If strictly and correctly implemented, mask-wearing can help reduce virus transmission with a high effectiveness of Level B, and sometimes, even Level A. The $t_{30\%}$ of mask-wearing is commonly greater than the lockdown of Level A and the shape of wave is less symmetrical. However, its effectiveness is dependent on public behavior (*20*) and can drop to Level C if people do not strictly abide by the rules. For example, Singapore adopted a strict mask-wearing policy that required 95% of the population to wear a mask outside their homes, starting from September 2020 (*20*). According to our model, such policies have the potential to achieve Level B effectiveness, with an average $t_{30\%}$ for approximately 30 days (Supplementary Table S1).

Level C Effectiveness — Night Curfews and Social Distancing

The effectiveness of less strict NPIs, such as social distancing and night curfew were studied (Supplementary Table S1) based on the data of 10 countries and regions, including Germany, Sweden, and New York State. The effectiveness of social distancing was not found to be highly satisfactory, even when accompanied by the night curfew policy, mainly fluctuating between Level B to C, with an average $t_{30\%}$ of approximately 44 and 48 days, respectively. By adopting these measures, a community will take at least twice as long to end the pandemic wave using less strict NPIs instead of lockdown.

By analyzing the history of the pandemic waves and the actual public response to the NPIs, we confirmed that leniency in implementing any anti-contagion policy would likely cause delays in pandemic control. Meanwhile rigorous execution of NPIs increases the braking force effectiveness. Consequently, when facing an outbreak, Level A measures should be implemented to promptly put the virus spread in control. Level B measures are also helpful but require additional time to curb the pandemic, whereas Level C NPIs have very limited contribution in this regard. Nevertheless, both Level B and C policies can be helpful for maintaining a low transmission level when the number of new cases decreases below $I_{5\%}$.

Braking Force Effect of Vaccines

With regard to investigating the effectiveness of vaccines in controlling the pandemic, our study focused on two countries, Israel and the United Arab Emirates (UAE), which had the highest vaccination ratios. We found that both these countries had inflection points of deceleration that were probably uncorrelated with the NPIs. The inflection point of the deceleration indicates the point at which the growth rate of epidemic cases has decreased, which in our model, is the date when the daily new cases start to decrease for a long period in the future. The inflection points of Israel took place on February 5, 2021, on which the braking force effect classification of its NPIs increased from Level C to Level B. For the UAE, despite its continuous use of Level C NPIs, an inflection point was still observed on February 24 (Figure 3).

Since antibodies develop approximately 10 to 14 days after the vaccination, we found that the day when the vaccine was given was also when both Israel and the UAE reached 50 vaccine doses administered (VDA) per 100 people in the total population. While Israel had NPIs such as lockdown, few NPIs were implemented in the UAE, such as partial border closing. Since the inflection point of Israel occurred after the lockdown was called off, and the NPIs of the UAE remained stable before and after the inflection

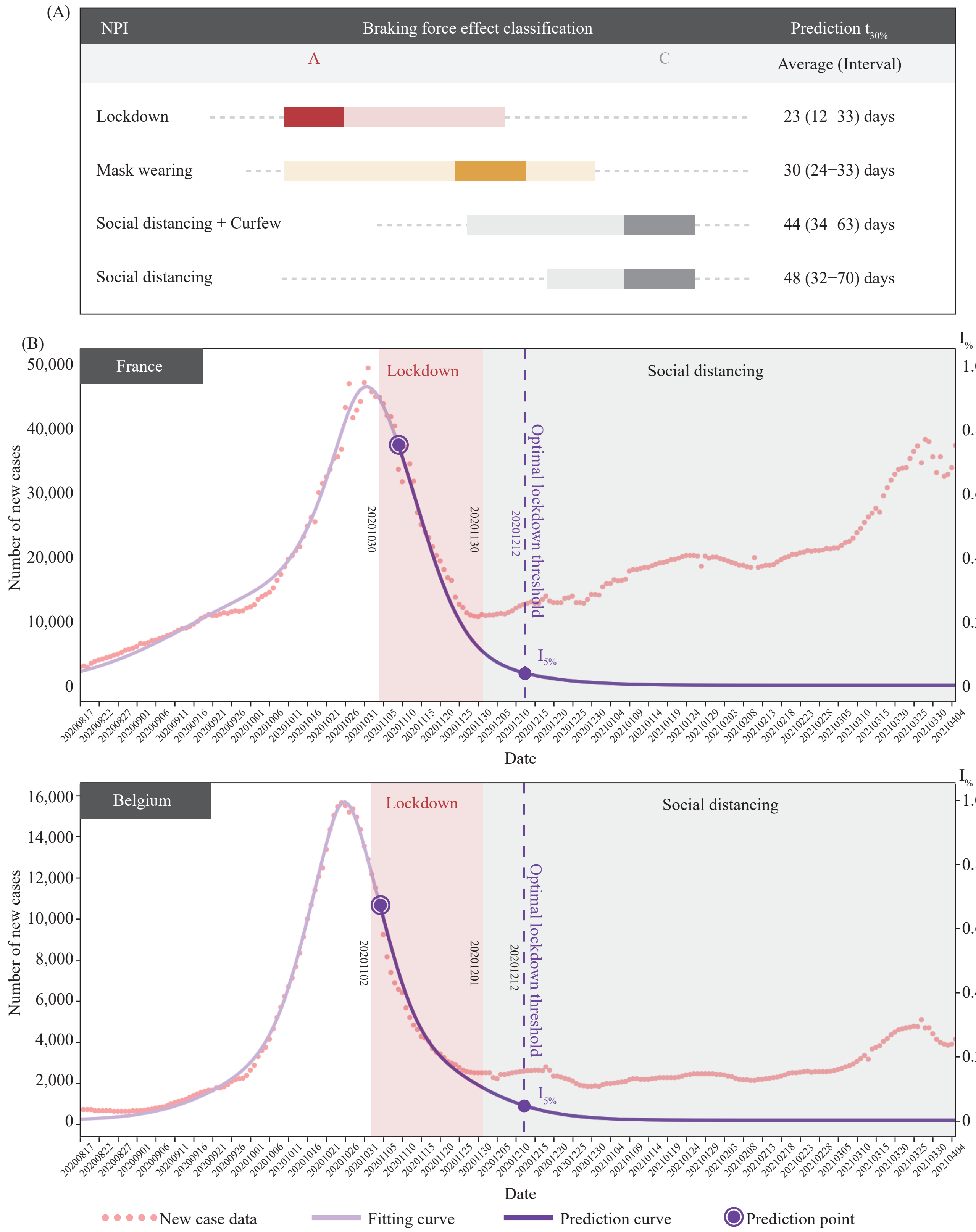

FIGURE 2. Non-pharmaceutical interventions (NPIs) classification and pandemic wave analysis. (A) Braking force effect classification of NPIs and their prediction $t_{30\%}$ value; (B) analysis of pandemic wave of France and Belgium.

Note: I%: A parameter to predict the number of new daily cases as a percentage relative to the highest number of daily cases during the current wave of the pandemic.

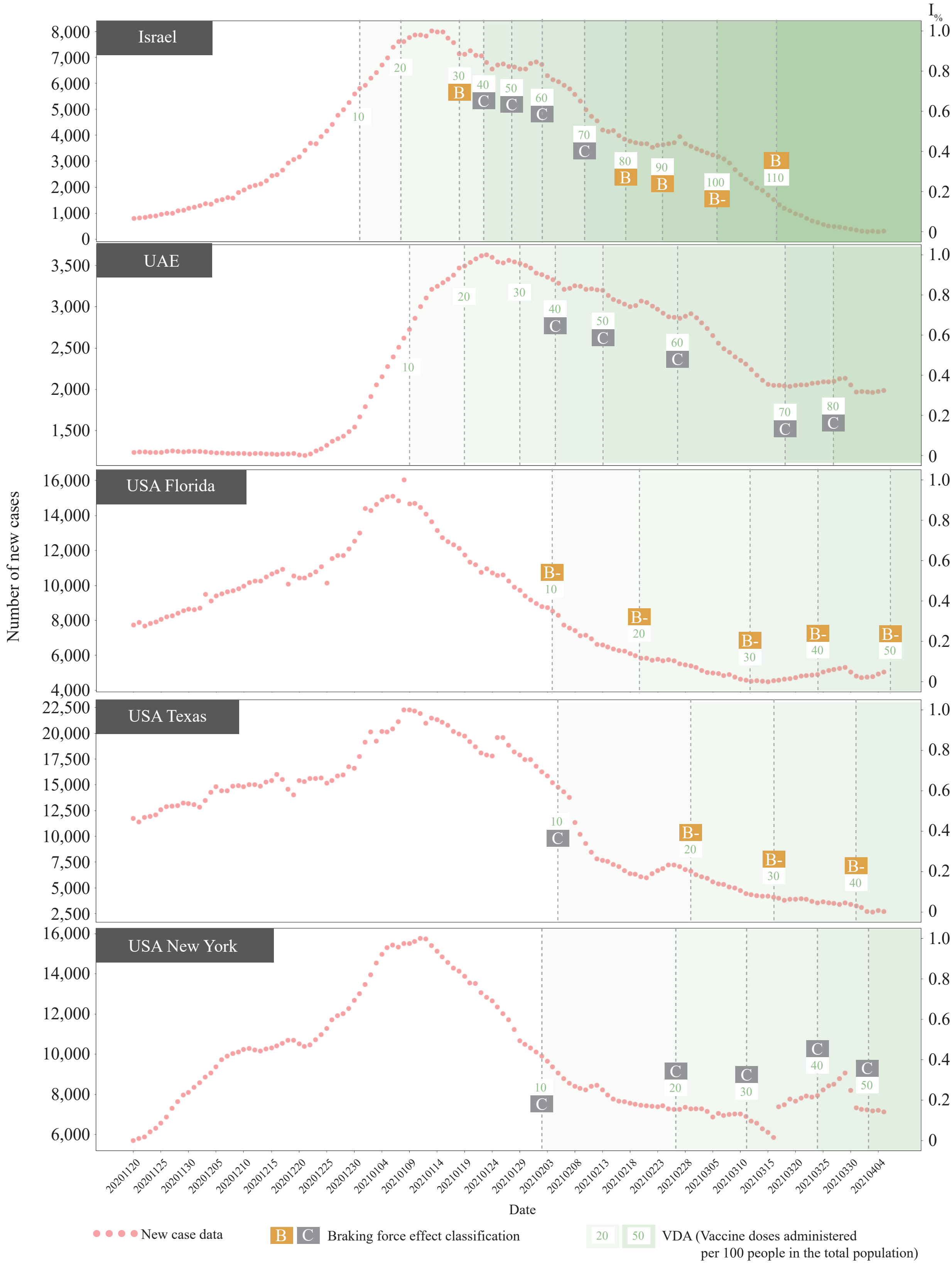

FIGURE 3. Braking Force Effectiveness classification of Israel, United Arab Emirates (UAE), and the United States (US) states of Florida, Texas, and New York with comparisons of different vaccination ratios.

Note: I%: A parameter to predict the number of new daily cases as a percentage relative to the highest number of daily cases during the current wave of the pandemic.

point, it was likely that the effectiveness of vaccination led to the inflection, so we could conclude that it is probably the vaccination played an important role in driving the wave to its inflection point.

In addition, Israel and UAE used different vaccines (Pfizer and Moderna for Israel, mRNA type and Sinopharm for UAE, inactivated type). These vaccines required two doses. Since the inflection point appeared synchronically around VDA=50, we could deduce that mRNA and inactivated vaccines showed an effect after VDA=50. Before that, the contribution of the vaccine to controlling the pandemic was uncertain.

After incorporating the daily new cases in Israel on February 27, 2021, our model projected that the virus spread could be controlled to reach $I_{5\%}$ on April 3; this finding showed good alignment with the later trajectory (Supplementary Figure S4, available in http://weekly.chinacdc.cn/). For the UAE, if the current anti-contagion policy continues, $I_{5\%}$ should be reached around June 5, 2021 (Supplementary Figure S4). Theoretically, continuous vaccination will result in herd immunization. Since different manufacturers stated that their current vaccines would provide at least six months of immunity, it is crucial to achieve herd immunity in 6 months.

When evaluating vaccine effectiveness, the US was also studied because this country had both a large number of new cases as well as vaccine doses that were administered. We focused on three states in the US: Florida, New York, and Texas, wherein different NPIs were implemented. To date, their VDA had not reached the delay of 50 + 14 days. Further, evident inflection points were observed. Notably, under similar VDA rates, the pandemic wave tendency and the braking force effectiveness classification of the three states were found to differ; thus, we can infer that the NPIs are the primary factors influencing the pandemic wave in the US.

DISCUSSION

Utilizing the Braking Force Model for COVID-19, we revealed the braking effect of NPIs and vaccines on the pandemic and provided a forecast method on when the pandemic could be controlled. Furthermore, this model also helps to propose a pandemic control strategy framework (Figure 4) when an outbreak occurs by implementing strict Level A NPIs, such as lockdown, to promptly and effectively curb virus transmission. In the first stage, the faster the spread of the pandemic can be restrained, the fewer the people who will be infected. Notably, the optimal threshold moment occurred when the number of new infections reduced to 5% of the summit of the wave, denoted $I_{5\%}$ (as predicted using our model); this was when the lockdown restrictions should be relaxed. Afterwards, less strict NPIs can be implemented to maintain the stability of the situation when the number of new cases is relatively low. In the second stage, there was a risk that the NPIs may become too lenient or relaxed, and

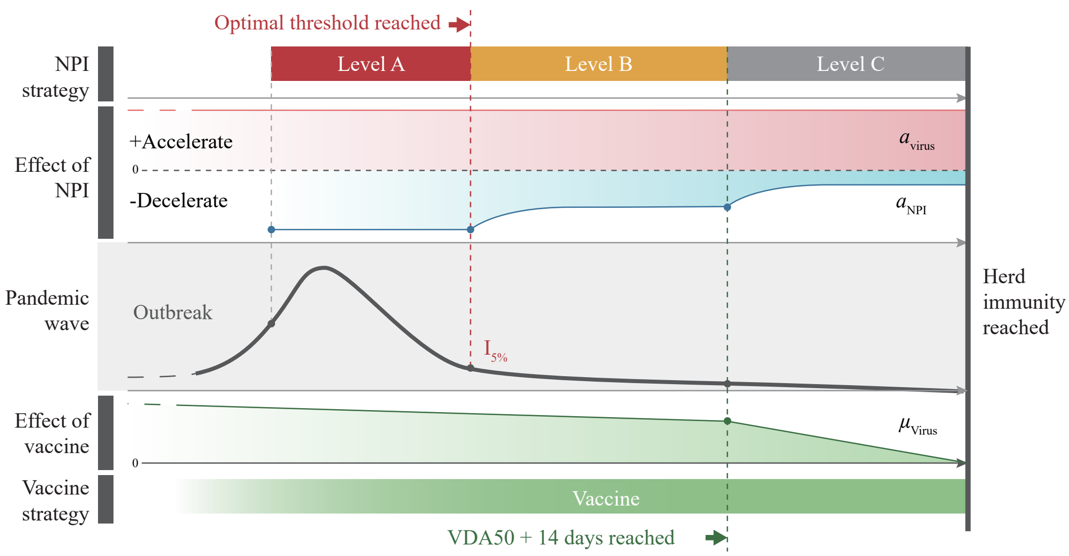

FIGURE 4. Anti-contagion strategy chart on COVID-19 obtained using the Braking Force Model.
Note: I%: A parameter to predict the number of new daily cases as a percentage relative to the highest number of daily cases during the current wave of the pandemic.
Abbreviation: NPI=non-pharmaceutical interventions.

this could lead to the sparking of a new outbreak.

To achieve herd immunity, vaccinating the majority of the population is paramount. Our study found that 14 days after VDA>50, the vaccine had a remarkably decelerating effect on controlling the pandemic. In the last stage, NPIs can be made more flexible, allowing the resumption of social life to a certain extent.

According to our model, the UK is a good example that demonstrates the effectiveness of vaccination. In its previous wave from last December, a new mutant virus in addition to cold weather posed a very high risk for a serious outbreak in the UK. However, the UK government imposed a strict lockdown policy until April 1, when new infections reduced to roughly $I_{5\%}$. At the same time, they continued their NPI measures, such as social distancing and mask-wearing and administered a large number of vaccines. The VDA of the UK has reached 50 and the vaccination effect can be increased if the vaccination can be done within a short period of time, aiming to achieve herd immunity

Projection and recommendation of the anti-contagion policy for several countries and regions by using the Braking Force Model can be found below (Supplementary Figures S5–S6, available in http://weekly.chinacdc.cn/). The limitation of this model is that it provides less information during the pandemic. However, this model offers insights into the dynamics of NPIs and vaccines in the pandemic with the help of peak or wave shape data analysis, and the results are easier to understand than those provided by conventional epidemic models.

The Braking Force model presented a new paradigm to predict the evolution of the COVID-19 pandemic. The effectiveness of different NPIs and vaccination were analyzed to help policymakers perform better forecasts with the measures they chose to implement. Our results showed that NPI intervention could likely only slow down the pandemic evolution but failed to eradicate the disease. Only vaccination had a higher likelihood of ending the pandemic, starting with VDA with approximately 50 + 14 days of delay for antibody production. The UK and Israel were close to the end of the national-level pandemic situation by successfully combining NPIs and high coverage of effective vaccinations.

Funding: Shenzhen-Hong Kong Science and Technology Innovation Cooperation Zone Shenzhen Park Project: HZQB-KCZYB-2020030, the National Natural Science Foundation of China No. 11875192; Chinese Academy of Sciences ANSO-SBA-2020-06; and Hong Kong Innovation and Technology Commission via the Hong Kong Branch of National Precious Metals Material Engineering Research Centre.

doi: 10.46234/ccdcw2021.195

Corresponding author: Jian Lu, jianlu@cityu.edu.hk.

[1] SJTU - Paristech Institute of Technology, Shanghai Jiao Tong University, Shanghai, China; [2] School of materials science and engineering, Shanghai Jiao Tong University, Shanghai, China; [3] School of Mechanical Engineering and Automation, Beihang University, Beijing, China; [4] Naval Medical Centre, Naval Medical University, Shanghai, China; [5] School of Data Science, City University of Hong Kong, Hong Kong, China; [6] Department of Biomedical Science, City University of Hong Kong, Hong Kong, China; [7] Hong Kong Branch of National Precious Metals Material Engineering Research Center (NPMM), City University of Hong Kong, Hong Kong, China.
[&] Joint first authors.

Submitted: August 16, 2021; Accepted: September 01, 2021

REFERENCES

1. World Health Organization. Coronavirus disease (COVID-19) weekly epidemiological update and weekly operational update. 2021. https: www.who.int/emergencies/diseases/novel-coronavirus-2019/situation-reports/. [2021-4-10].
2. Saad-Roy CM, Wagner CE, Baker RE, Morris SE, Farrar J, Graham AL, et al. Immune life history, vaccination, and the dynamics of SARS-CoV-2 over the next 5 years. Science 2020;370(6518):811 – 8. http://dx.doi.org/10.1126/science.abd7343.
3. Cobey S. Modeling infectious disease dynamics. Science 2020;368 (6492):713 – 4. http://dx.doi.org/10.1126/science.abb5659.
4. Pei S, Kandula S, Shaman J. Differential effects of intervention timing on COVID-19 spread in the United States. Sci Adv 2020;6 (49):eabd6370. http://dx.doi.org/10.1126/SCIADV.ABD6370.
5. Davies NG, Abbott S, Barnard RC, Jarvis CI, Kucharski AJ, Munday JD, et al. Estimated transmissibility and impact of SARS-CoV-2 lineage B.1.1.7 in England. Science 2021;372(6538):eabg3055. http://dx.doi.org/10.1126/science.abg3055.
6. Lai SJ, Ruktanonchai NW, Zhou LC, Prosper O, Luo W, Floyd JR, et al. Effect of non-pharmaceutical interventions to contain COVID-19 in China. Nature 2020;585(7825):410 – 3. http://dx.doi.org/10.1038/s41586-020-2293-x.
7. Flaxman S, Mishra S, Gandy A, Unwin HJT, Mellan TA, Coupland H, et al. Estimating the effects of non-pharmaceutical interventions on COVID-19 in Europe. Nature 2020;584(7820):257 – 61. http://dx.doi.org/10.1038/s41586-020-2405-7.
8. Soltesz K, Gustafsson F, Timpka T, Jaldén J, Jidling C, Heimerson A, et al. The effect of interventions on COVID-19. Nature 2020;588 (7839):E26 – 28. http://dx.doi.org/10.1038/s41586-020-3025-y.
9. Hsiang S, Allen D, Annan-Phan S, Bell K, Bolliger I, Chong T, et al. The effect of large-scale anti-contagion policies on the COVID-19 pandemic. Nature 2020;584(7820):262 – 7. http://dx.doi.org/10.1038/s41586-020-2404-8.
10. Mathieu E, Ritchie H, Roser M. Our World in Data is now tracking Coronavirus (COVID-19) vaccinations across the world. 2021. https://ourworldindata.org/covid-vaccination-dataset. [2021-4-10].
11. Pollán M, Pérez-Gómez B, Pastor-Barriuso R, Oteo J, Hernán MA, Pérez-Olmeda M, et al. Prevalence of SARS-CoV-2 in Spain (ENE-COVID): a nationwide, population-based seroepidemiological study. Lancet 2020;396(10250):535 – 44. http://dx.doi.org/10.1016/S0140-6736(20)31483-5.
12. Chang S, Pierson E, Koh PW, Gerardin J, Redbird B, Grusky D, et al. Mobility network models of COVID-19 explain inequities and inform reopening. Nature 2021;589(7840):82 – 7. http://dx.doi.org/10.1038/s41586-020-2923-3.

13. Kraemer MUG, Yang CH, Gutierrez B, Wu CH, Klein B, Pigott DM, et al. The effect of human mobility and control measures on the COVID-19 epidemic in China. Science 2020;368(6490):493 – 7. http://dx.doi.org/10.1126/science.abb4218.
14. Tian HY, Liu YH, Li YD, Wu CH, Chen B, Kraemer MUG, et al. An investigation of transmission control measures during the first 50 days of the COVID-19 epidemic in China. Science 2020;368(6491):638 – 42. http://dx.doi.org/10.1126/science.abb6105.
15. Walker PGT, Whittaker C, Watson OJ, Baguelin M, Winskill P, Hamlet A, et al. The impact of COVID-19 and strategies for mitigation and suppression in low- and middle-income countries. Science 2020;369(6502):413 – 22. http://dx.doi.org/10.1126/science.abc0035.
16. Britton T, Ball F, Trapman P. A mathematical model reveals the influence of population heterogeneity on herd immunity to SARS-CoV-2. Science 2020;369(6505):846 – 9. http://dx.doi.org/10.1126/science.abc6810.
17. Lu J. A new, simple projection model for COVID-19 pandemic. medRxiv 2020. http://dx.doi.org/10.1101/2020.03.21.20039867.
18. Sun KY, Wang W, Gao LD, Wang Y, Luo KW, Ren LS, et al. Transmission heterogeneities, kinetics, and controllability of SARS-CoV-2. Science 2021;371(6526):eabe2424. http://dx.doi.org/10.1126/science.abe2424.
19. Blacatnik School of Government University, University of Oxford. COVID-19 government response tracker. 2021. https://www.bsg.ox.ac.uk/research/research-projects/covid-19-government-response-tracker. [2021-4-10].
20. Imperial College London. COVID-19 behavior tracker. 2021. https://www.imperial.ac.uk/centre-for-health-policy/our-work/our-response-to-covid-19/covid-19-behaviour-tracker/. [2021-4-10].

Supplementary Materials

The structure of Materials and Methods is as follows: we first introduce the construction process of our model-specific database in the "Datasets" section. Then, in the "Model" section, the origin of final parameter interval for different classes is explained. Finally, in the "Classification and forecast method" section, the detailed procedure for classifying the observed curve of daily reported cases and predicting the development is presented.

Datasets

Storage of epidemic COVID-19 curve

From the dataset of World Health Organization (*1*) and Our World in Data (*2*), we collected and saved the daily new cases of COVID-19 covering the data from January 22, 2020 to April 9, 2021 from more than 60 countries and regions. The date is accurate to the day, however, due to different conditions, statistical methods and administrative implementation between countries, the data vary greatly in form and in scale. In our study, these data were presented in form of curves by setting date as horizontal axis and the number of daily new cases as vertical axis.

Process of epidemic COVID-19 curve

In order to facilitate the extraction and the analysis of features of the original data, a preliminary process was introduced. The pre-processing contained two steps. The first step was smoothing the data. The number of each day was smoothed by the data of seven days before and after, which means we replaced the number of that day by the average value of the seven days. This procedure can partly remove the noise in the data and help reflect the trend. Secondly, we divided the data of each country/region into a minor level: waves. Each wave represents a round of outbreak and mitigation of COVID-19. The following rule were used to identify a wave: it starts from the closest

SUPPLEMENTARY TABLE S1. Classification of different non-pharmaceutical interventions of history wave and their forecast parameter $t_{30\%}$.

Non-pharmaceutical interventions	Country/Region	Period	Classification	$t_{30\%}$	Average $t_{30\%}$
Lockdown	France	2020.8–2020.12	A	23	23
	South Africa	2020.9–2021.3	A	12	
	Belgium	2020.8–2020.12	A	14	
	Austria	2020.8–2021.1	A–	33	
	UK	2020.9–2021.3	B	32	
Mask wearing	The Republic of Korea *	2020.2– 2020.4	A	12	/
	Hong Kong *	2020.3– 2020.5	A–	16	
	Japan *	2020.1– 2020.3	B	22	
	Japan	2020.9–2021.1	B	24	30
	The Republic of Korea	2020.10–2021.2	B–	33	
	Spain	2020.7–2020.11	B–	32	
Social distancing + Curfew	Texas	2020.9–2021.3	B	34	44
	Hungary	2020.8–2021.1	B–	44	
	Illinois	2020.9–2021.1	C	42	
	Florida	2020.9–2021.2	C	35	
	Slovenia	2020.8–2021.3	C	63	
Social distancing	Iowa	2020.9–2021.1	B–	32	48
	New York	2020.9–2021.2	B–	57	
	Germany	2020.8–2021.2	B–	44	
	Switzerland	2020.8–2021.2	C	35	
	Sweden	2020.9–2021.2	C	70	

* The history waves were not counted into the average value of $t_{30\%}$.

inflection point before its augmentation and ends on the closest inflection point after its decline. The inflection point was defined as the points between two local maximums of the smoothed data around which the data remained stable. The following research will mainly focus on the waves of the smoothed data of all the sample countries.

Classification of epidemic curve in training set

We subdivided the original epidemic data into wave-based data and randomly divided them into a training set and a test set at a ratio of 8∶2. The training set was used to build the model, and the test set was used to test the validity of the model. We manually classified the epidemic wave curve in the training set into three levels: A, B, and C based on the pandemic control efficiency in previous text, part "Classification and forecast of the braking force effect" with level A being the highest and level C being the lowest (Supplementary Figure S1). Therefore, the database contained the classified training set and the test set to be verified. The data in both sets were based on the smoothed epidemic curve data of each wave in each sample country/region.

Model

Initial parameter intervals

To obtain the initial parameter interval of each Braking Force Effect Level, epidemic curves in training set were processed. Since the Gaussian function was frequently used to describe the natural phenomenon including the spread of infectious disease, while the epidemic curve usually has strong fluctuation, our study applied a linear combination of three Gaussian functions to fit the epidemic curve, which could be expressed as follow:

$$f(x) = a_1 \frac{e^{-(x-\mu_1)^2}}{2\sigma_1^2} + a_2 \frac{e^{-(x-\mu_2)^2}}{2\sigma_2^2} + a_3 \frac{e^{-(x-\mu_3)^2}}{2\sigma_3^2}$$

In which, a_i, μ_i, σ_i are the amplitudes, mean value and standard deviation of each Gaussian function. Loss function is defined as the mean-square error $\delta(X) = \sum_{i=1}^{n} \frac{(y_i - f(x_i))^2}{n}$ in which n is number of points in the origin epidemic curve, x_i and y_i are the abscissa and ordinate of the corresponding point.

Since there were nine parameters to fit, an algorithm combining the Bayesian algorithm and gradient descent method was proposed to enhance the speed and accuracy, in which the Bayesian algorithm could quickly find a feasible solution close to the optimal solution in the search space and the gradient descent method was used to effectively approximate the optimal solution.

Through the above method, the epidemic wave in the training set could be quickly and accurately fitted by the linear combination of three Gaussian functions. After each fitting, it generated a set of data containing nine corresponding parameters, therefore the initial parameter intervals of each level were formed.

Final parameter intervals. Albeit the initial parameter had been found, the classification and forecast capability of the model was not satisfied. The reason was that the nine independent parameters intervals cannot effectively represent the three classes of epidemic curve. Therefore, feature parameters have been setup in order to reduce the

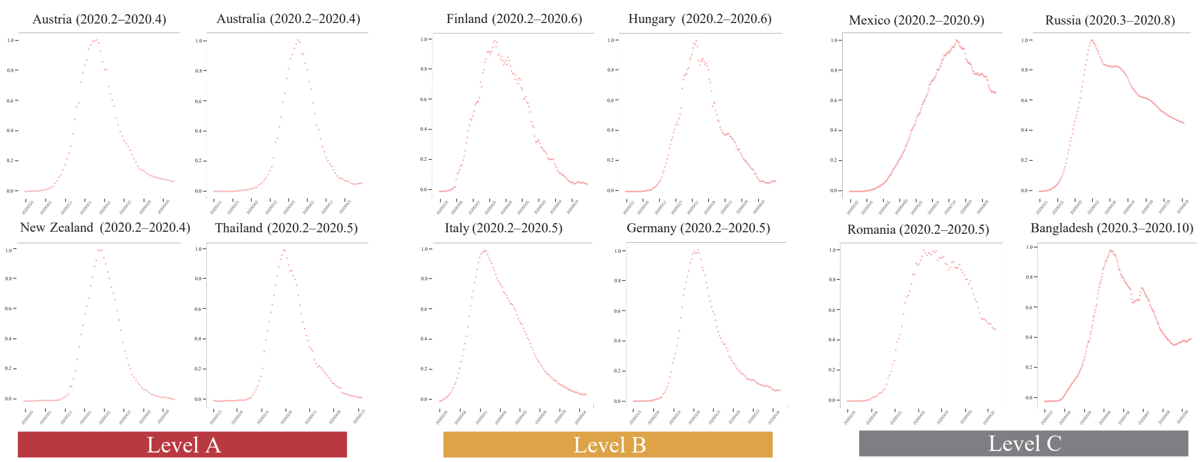

SUPPLEMENTARY FIGURE S1. Samples of pandemic wave classified into braking force effect level A, B, and C according to the pandemic control effectiveness.

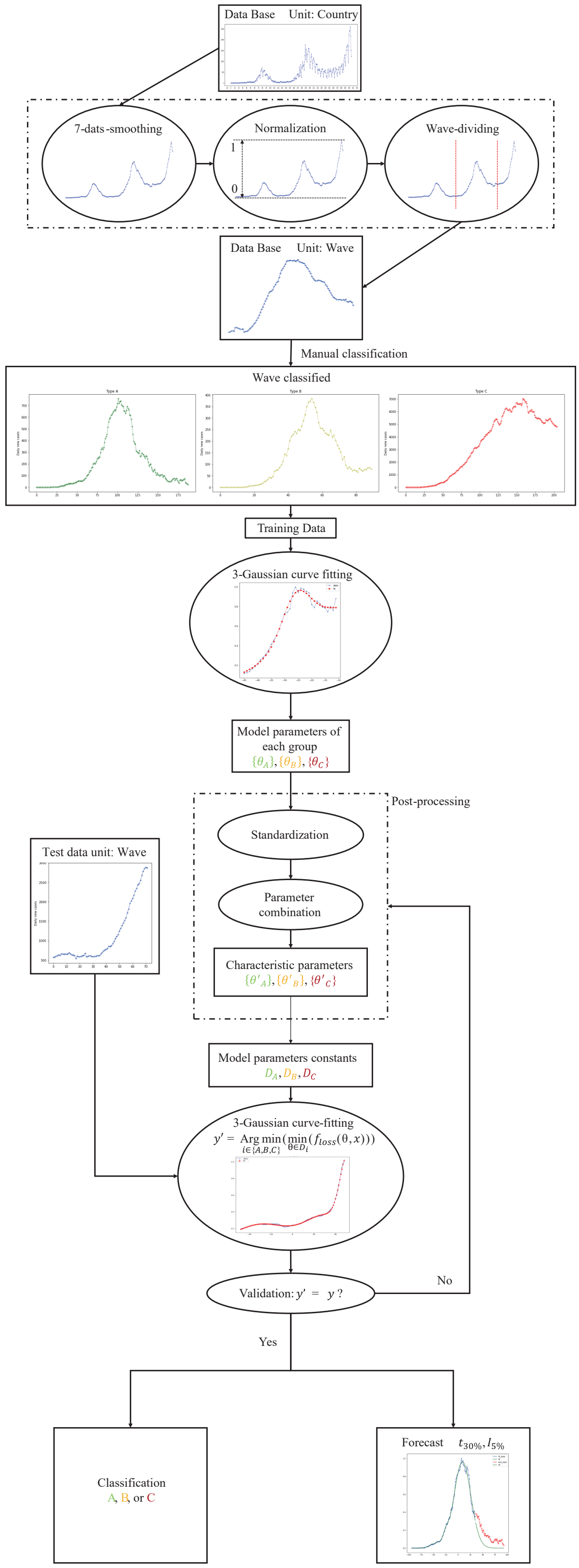

SUPPLEMENTARY FIGURE S2. Flow chart of classification and forecast with detail information of the Braking Force Effect model above the caption.

Note: I%: A parameter to predict the number of new daily cases as a percentage relative to the highest number of daily cases during the current wave of the pandemic.

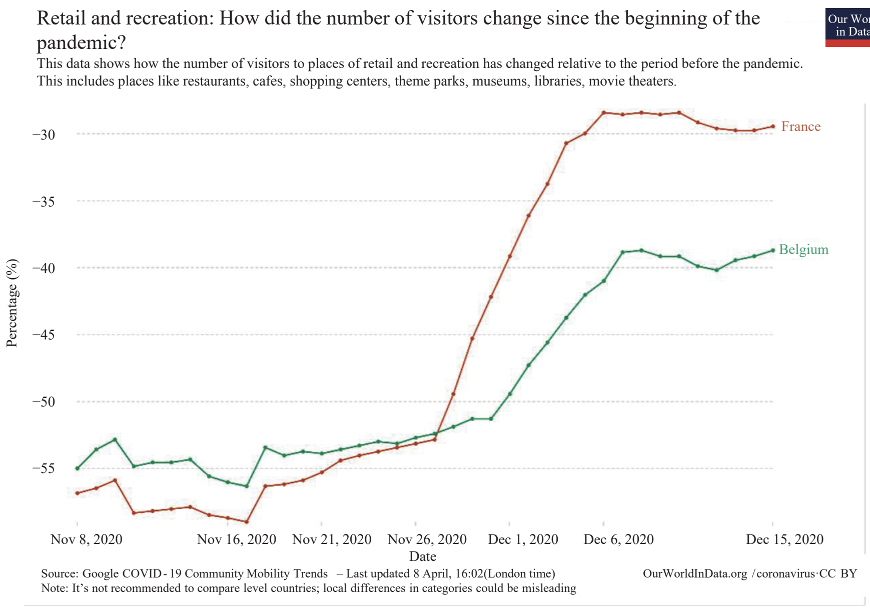

SUPPLEMENTARY FIGURE S3. Community mobility trends of France and Belgium during the period of November 8 to December 15, 2020 (*1*).

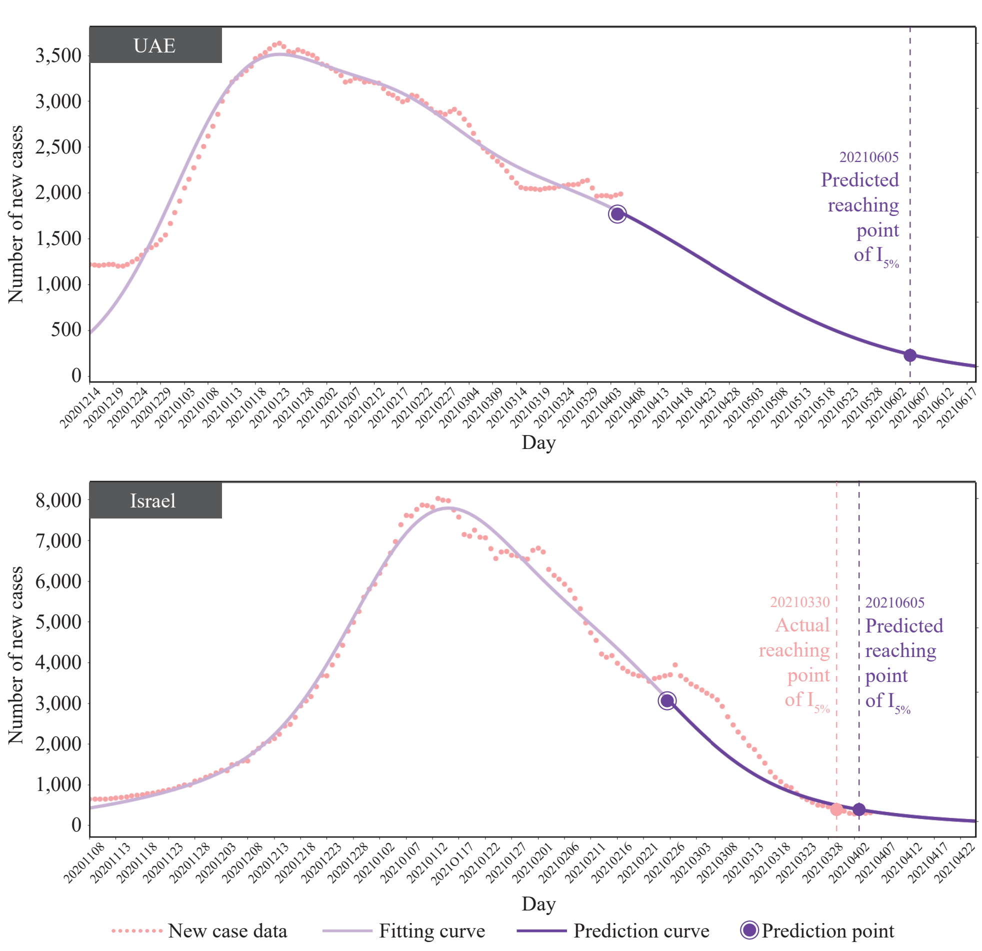

SUPPLEMENTARY FIGURE S4. Forecast of current pandemic wave of Israel and UAE.

Note: I%: A parameter to predict the number of new daily cases as a percentage relative to the highest number of daily cases during the current wave of the pandemic.

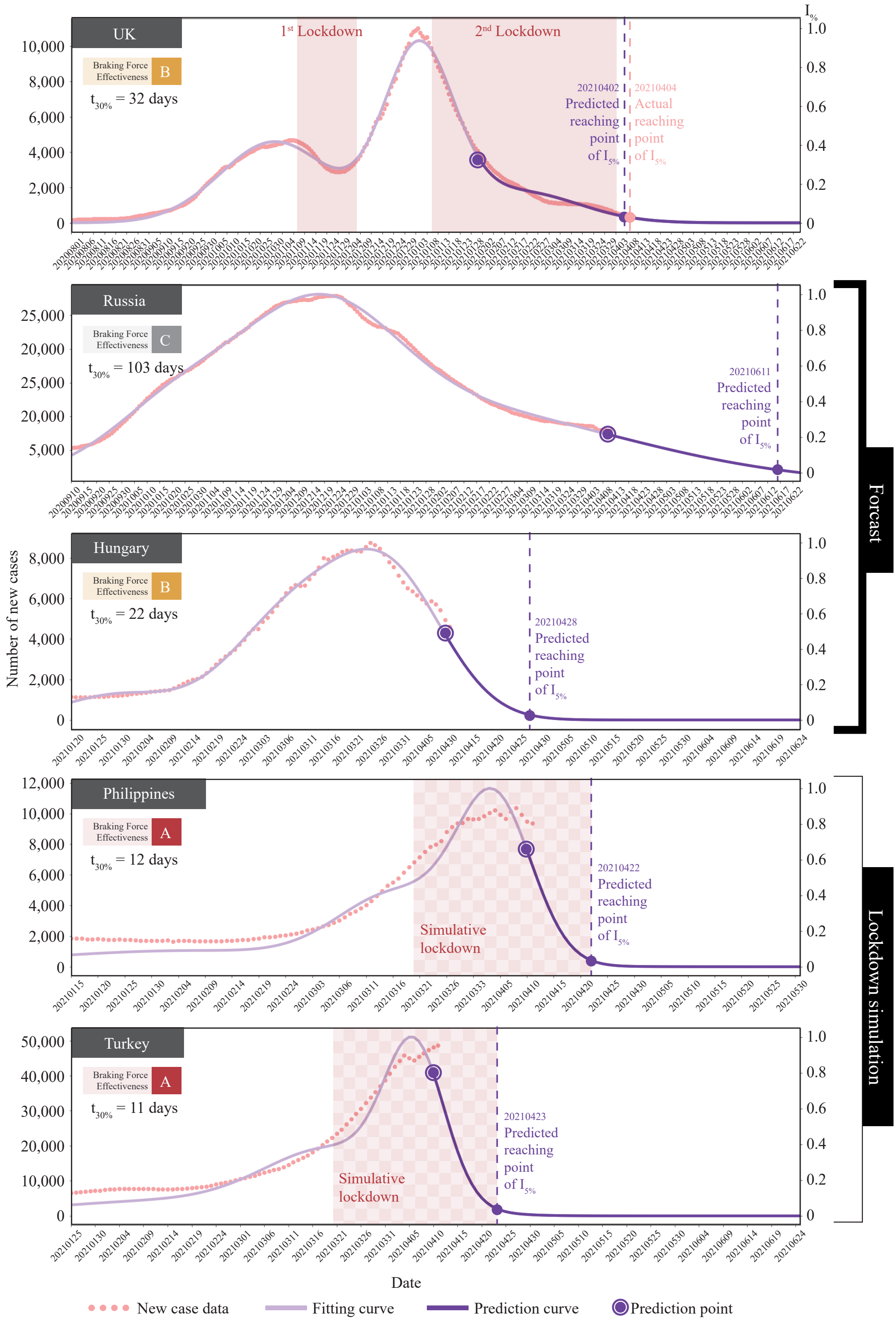

SUPPLEMENTARY FIGURE S5. “Braking Force Effect” model application. (A) “Braking Force Effect” model application to UK; (B) forecast of COVID-19 new case of Russia and Hungary. (C) “Braking force effect” model simulation of new case number tendency if The Philippines and Turkey implement Level A NPIs.

Note: I%: A parameter to predict the number of new daily cases as a percentage relative to the highest number of daily cases during the current wave of the pandemic.

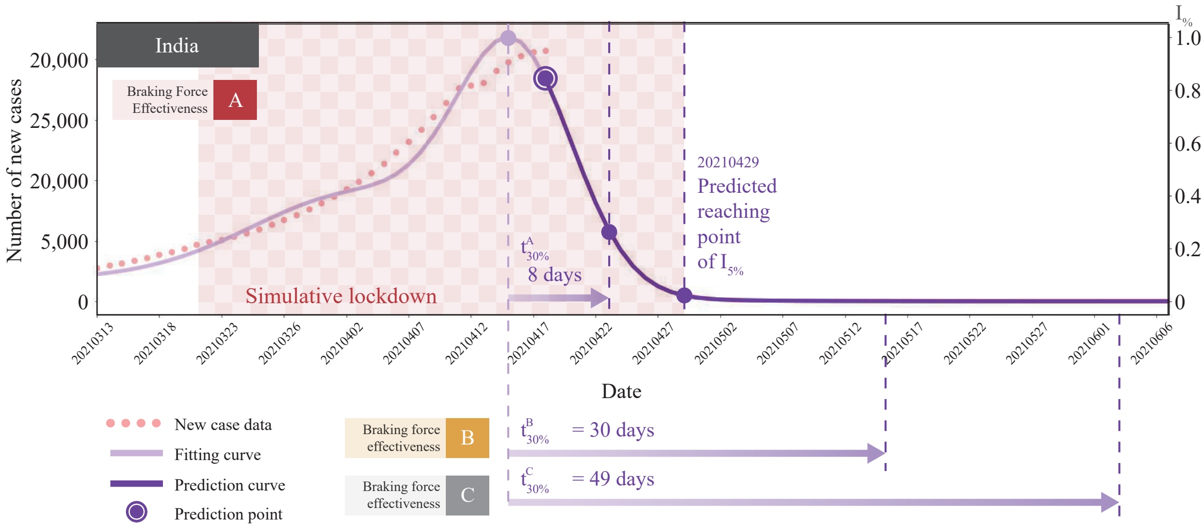

SUPPLEMENTARY FIGURE S6. “Braking Force Effect” model simulation of new case number tendency for India with different Braking Force Effectiveness.

Note: I%: A parameter to predict the number of new daily cases as a percentage relative to the highest number of daily cases during the current wave of the pandemic.

initial parameter interval as well as to improve the classification and forecast capabilities of the model.

The feature parameters are a_1, a_{2_r}, a_{3_r}, μ_{1_n}, μ_{2_n}, μ_{3_n}, σ_{1_n}, σ_{2_r}, σ_{3_r}, where $a_{i_r} = {}^{a_i}\!/_{a_1}$, $i = 2, 3$; $\mu_{i_r} = {}^{a_i}\!/_{N}$, $i = 1, 2, 3$; $\sigma_{1_n} = {}^{\sigma_1}\!/_{N}$; $\sigma_{i_r} = {}^{\sigma_i}\!/_{\sigma_1}$, $i = 2, 3$ and N is the number of sampling points. The selection of index i is to evaluate the influence of the second and third peak to the main peak to estimate the fluctuation of the epidemic curve. The selection of index n is to limit the range of μ and σ when processing a long-term epidemic wave. Through the limitation of these new feature parameters, the final parameter intervals were calculated, and it was found that their range is greatly limited comparing to the initial parameter intervals. As a result, the overlap between each class in the nine-dimension space was reduced, the capability of classification was effectively improved.

Characteristic parameters

Besides the feature parameters used to calculate the final parameter interval mentioned above, characteristic parameters have been setup to assist the classification. The boxplot was used to exploit these parameters in order to distinguish the interval of each level. Characteristic parameters that meet the above requirement could be expressed below which were mainly related to a_1, a_2, a_3, σ_2, because these parameters would greatly influence the fluctuation of epidemic curve.

$$a_{sqr} = \frac{\sqrt{a_2^2 + a_3^2}}{a_1}, \quad a_{3_r} = \frac{a_3}{a_1}, \quad a_{23_r} = \frac{a_2 \times a_3}{a_1^2},$$

$$t_2 = a_{23_r} \times a_{2_r} \times \sigma_{2_r}, etc.$$

These characteristic parameters of epidemic wave in the training set of each level presented a certain interval, and the scatter chart between 2 characteristic parameters, e.g., a_{sqr} *Vs* a_{3_r} or a_{23_r} *Vs* t_2, presented a characteristic spatial distribution and slope range. By analyzing the characteristic parameters and the scatter charts, we can classify the types of one epidemic wave.

Classification and Forecast Method

Classification method

To classify the existing curve of each wave according to the criteria mentioned in the “Datasets” section, our standard procedure was divided into three steps. First, fit respectively the existing wave within the final parameter intervals of three levels obtained in the “Model adjustment” part by using the linear combination of three Gaussian functions. Second, classify preliminarily the waves by choosing the level with the smallest chi-squared value, if the chi-squared value was almost equally to two neighbor level, e.g. “A and B” and “B and C,” the wave would be classified as A– and B–, respectively. Third, calculate the corresponding characteristic parameters and their relative scatter charts. By comparing the relative distance to other points of three levels and the slope from the position to the origin, the auxiliary result could be obtained to judge quantitatively whether the preliminary classification is reasonable. If the result between preliminary and auxiliary classification was the same then the former judgment would be accepted; otherwise, the wave would be reclassified. By repeating the classification until they were agreed, the final classification could be obtained, including A, A–, B, B–, C.

Forecast Method

To predict the number of daily reported cases, the nine parameters of the linear combination of three Gaussian function were firstly calculated according to the procedure in "Classification Method" part. The wave thus could be extended as the forecast result. The flow chart of classification and forecast with detail information of the "braking force effect" model is presented in Supplementary Figure S3.

During the forecast, a variable named $t_{30\%}$ was defined for indicating the decrease velocity of pandemic wave, unit of days, presented as the number of days required to decrease from the summit of wave to its 30%. We supposed a wave normalized as $w : [\![0, N]\!] \rightarrow [0, 1]$ and the $t_{30\%}$ defined as:

$$t_{30\%} = min(\{n \in [\![0, N]\!], \forall i \in [\![n, N]\!], w(i) \leq 0.3 \times max(w)\})$$

A wave with a smaller $t_{30\%}$ value means the pandemic have been efficiently controlled. History waves of different countries/regions with different implemented NPIs were classified and listed in Supplementary Table S1. $t_{30\%}$ of each history wave were calculated, and the average $t_{30\%}$ of each corresponding NPIs are presented in the table. Average value of $t_{30\%}$ were only for the history wave after July 2020, considering that in most parts of the world, the new case number of the COVID-19 after July 2020 was much higher than before.

REFERENCES

1. World Health Organization. Coronavirus disease (COVID-19) weekly epidemiological update and weekly operational update. 2021. https:www.who.int/emergencies/diseases/novel-coronavirus-2019/situation-reports/. [2021-4-10].
2. Mathieu E, Ritchie H, Roser M. Our World in Data is now tracking Coronavirus (COVID-19) vaccinations across the world. 2021. https://ourworldindata.org/covid-vaccination-dataset. [2021-4-10].

Indexed by PubMed Central (PMC) and Emerging Sources Citation Index (ESCI).

The inauguration of *China CDC Weekly* is in part supported by Project for Enhancing International Impact of China STM Journals Category D (PIIJ2-D-04-(2018)) of China Association for Science and Technology (CAST).

CCDC weekly

Vol. 3 No. 40 Oct. 8, 2021

Responsible Authority

National Health Commission of the People's Republic of China

Sponsor

Chinese Center for Disease Control and Prevention

Editing and Publishing

China CDC Weekly Editorial Office

No.155 Changbai Road, Changping District, Beijing, China

Tel: 86-10-63150501, 63150701

Email: weekly@chinacdc.cn

CSSN

ISSN 2096-7071

CN 10-1629/R1